



Norges miljø- og  
biovitenskapelige  
universitet

**Master's Thesis 2024 60 ECTS**

The Faculty of Environmental Sciences and Natural Resources  
Management, MINA

# **Application and Optimization of a Method for Determination of Stable Boron Isotope Ratios in Various Aqueous Matrices Using Inductively Coupled Plasma Mass Spectrometry**

Julianne Hem



## Abstract

This thesis aims to optimize and apply an existing method for boron isotope analysis to various aqueous matrices with differing boron concentrations, as part of the MetroPOEM project's goal to develop SI-traceable methods for stable isotope ratio measurements. The method builds on the work of de la Vega et al. 2020, utilizing automated chromatography with the ESI prepFAST system and Amberlite IRA743 resin, coupled with Multicollector-Inductively Coupled Plasma Mass Spectrometry (MC-ICP-MS). Key challenges include potential isotope fractionation during chromatographic separation and instrumental analysis, mass bias in the ICP-MS, and boron's adhesive properties, which result in memory effects.

Boron has two stable isotopes,  $^{10}\text{B}$  and  $^{11}\text{B}$ , which undergo significant fractionation in nature because of their 10% relative mass difference, making boron isotope ratios valuable as a geochemical tracer. A total of 372 measurements across 299 unique samples, spanning nine water categories, were validated against four research criteria:

1. Achieving a limit of detection (LOD) below the atomic boron concentration of 3.0 ng/mL.
2. Maintaining a standard deviation below 5‰ for replicate  $\delta^{11}\text{B}$ -values
3. Ensuring recovery rates from 95–105% to avoid fractionation
4. Achieving a standard deviation of less than 1‰ for the measured  $\delta^{11}\text{B}$ -values of the certified reference material ERM-AE123, compared to its theoretical  $\delta^{11}\text{B}$ -value of  $-40 \pm 0.60\text{‰}$ .

These criteria assessed the method's sensitivity, precision, yield and accuracy, overall validating the method's precision and accuracy.

The research question, "Will the measured boron concentrations and  $\delta^{11}\text{B}$ -values align with the theoretical values for each of the aqueous matrices?" was successfully addressed. The method achieved an LOD of 1.4 ng/mL, fulfilling Research Criteria 1 and demonstrating high sensitivity. However, recovery rates were inconsistent and generally below 100%, failing to meet Research Criteria 3, and possibly contributed to failing the precision criteria of replicate  $\delta^{11}\text{B}$ -values being below 5‰ standard deviations, and the measured  $\delta^{11}\text{B}$ -values of ERM-AE123 exceeding 1‰ standard deviation from the theoretical  $\delta$ -value. Failing to meet the research criteria, indicates that further optimization is necessary. Specifically, increasing the sample pH to convert more boron into borate anions could potentially improve binding to the column and facilitate a more efficient elution step, leading to better recovery rates.

## Sammendrag

Denne masteroppgaven har som mål å optimalisere og anvende en eksisterende metode for analyse av borisotoper på ulike vannmatriser med varierende borkonsentrasjoner, som en del av MetroPOEM-prosjektets mål om å utvikle SI-sporbare metoder for måling av stabile isotopforhold. Metoden bygger på arbeidet til de la Vega et al. (2020) og benytter seg av automatisert kromatografi, et ESI prepFAST-system, med Amberlite IRA743-resin, kombinert med multikollektor induktivt koblet plasma massespektrometri (MC-ICP-MS). Sentrale utfordringer inkluderer mulig isotopfraksjonering under den kromatografiske separasjonen og instrumentanalyse, massebias i ICP-MS, samt bors adhesjonsegenskaper som fører til minneeffekter. Bor har to stabile isotoper,  $^{10}\text{B}$  og  $^{11}\text{B}$ , som gjennomgår betydelig fraksjonering i naturen på grunn av deres relative masseforskjell på 10 %, noe som gjør borisotopforhold verdifulle i geokjemisk forskning. Totalt ble 372 målinger fordelt på 299 unike prøver, fordelt på ni vannkategorier, validert mot fire valideringskriterier.

1. Å oppnå en deteksjonsgrense (LOD) under den atomiske borkonsentrasjonen på 3.0 ng/mL.
2. Opprettholde en standardavvik under 5‰ for replikater av  $\delta^{11}\text{B}$ -verdier.
3. Sikre utbytte mellom 95–105 % for å unngå fraksjonering.
4. Å oppnå et standardavvik på mindre enn 1‰ for de målte  $\delta^{11}\text{B}$ -verdiene til det sertifiserte referansematerialet ERM-AE123, sammenlignet med dets teoretiske  $\delta^{11}\text{B}$ -verdi på  $-40 \pm 0,60\%$ .

Disse kriteriene vurderte metodens sensitivitet, presisjon, utbytte og nøyaktighet, og validerte samlet sett metodens presisjon og nøyaktighet. Forskningsspørsmålet "Vil de målte borkonsentrasjonene og  $\delta^{11}\text{B}$ -verdiene samsvare med de teoretiske verdiene for hver av vannmatrisene?" ble innfridd. Metoden oppnådde en LOD på 1.4 ng/mL, og oppfylte kriterium 1, noe som demonstrerte høy sensitivitet i metoden. Derimot var utbytteverdiene varierende og generelt under 100 %, noe som ikke oppfylte kriterium 3. Dette kan ha bidratt til at presisjonskriteriene for replikerte  $\delta^{11}\text{B}$ -verdier, med et standardavvik under 5‰, samt de målte  $\delta^{11}\text{B}$ -verdiene for ERM-AE123, overskred 1‰ standardavvik fra den teoretiske  $\delta$ -verdien. At kriteriene ikke ble oppfylt, indikerer at videre optimalisering er nødvendig. Potensielt kan en økning av prøvenes pH for å gjøre mer bor til boratanioner forbedre binding til kolonnen og legge til rette for et mer effektivt elueringssteg, noe som kan øke utbytteverdiene.

## **Preface**

This thesis was a part of the EURAMET project 21GRD09 Metrology for the harmonization of measurements of environmental pollutants in Europe (METROpoem). All laboratory work has been carried out at the stable isotope laboratory of the Institute for Energy Technology in Kjeller, Lillestrøm, in collaboration with the Norwegian University of Life Sciences (NMBU). 84 boron water samples were measured personally at IFE, and 288 samples were analyzed using the method by my supervisor as a part of the laboratory's daily activities.

I would like to thank my supervisors Christian Schöpke (IFE/NMBU) for helping me plan and execute the practical laboratory work at IFE, as well as giving me valuable help in writing and analyzing data, and Professor Lindis Skipperud (NMBU) for supporting me in writing this thesis. I also want to thank Simon Mark Jerome for his help in data analysis and looking over this thesis in the final week.

I want to thank the people at the stable isotope laboratory at IFE for a good atmosphere, kindness and support at the laboratory. Also, I would like to thank my family for always supporting me with what I do, and encouraging me throughout my studies.

Julianne Hem

Ås, Norway, NMBU, 12.12.2024

## Terms and abbreviations

<b><math>\delta^{11}\text{B}</math>-value</b>	Per mille difference in $^{11}\text{B}$ relative to NIST <sub>951a</sub>
<b>CRM</b>	Certified reference material
<b>HR-ICP-MS</b>	High Resolution Inductively Coupled Plasma Mass Spectrometer
<b>ICP-MS</b>	Inductively Coupled Plasma Mass Spectrometer
<b>IFE</b>	Institutt for energiteknikk/ Institute for Energy Technology
<b>LOD/LOQ</b>	Limit of Detection & Limit of Quantification
<b>MC-ICP-MS</b>	Multicollector Inductively Coupled Plasma Mass Spectrometer
<b>METROpoem</b>	EURAMET project 21GRD09 Metrology for the harmonization of measurements of environmental pollutants in Europe
<b>NIST<sub>951a</sub></b>	The reference material used to define the $\delta^{11}\text{B}$ scale, its own $\delta^{11}\text{B}$ -value assigned to 0‰ <sub>NIST951a</sub>
<b>NMBU</b>	Norges miljø- og biovitenskapelige universitet/ Norwegian University of Life Sciences
<b>PFA</b>	Perfluoroalkoxy alkanes
<b>SIMS</b>	Secondary Ion Mass Spectrometer
<b>TIMS</b>	Thermal Ionization Mass Spectrometer

# Table of contents

<b>1. Introduction .....</b>	<b>1</b>
1.1 <i>The Objective of This Thesis.....</i>	<i>1</i>
1.2 <i>Research Questions and Research Criteria.....</i>	<i>2</i>
<b>2. Theory .....</b>	<b>3</b>
2.1 <i>Boron Isotopes, Fractionation and Applications .....</i>	<i>3</i>
2.2 <i>Automated Chromatography with prepFAST and IRA743.....</i>	<i>7</i>
2.3 <i>Inductively Coupled Plasma Mass Spectrometry .....</i>	<i>10</i>
2.4 <i>Measurements and Uncertainty.....</i>	<i>11</i>
2.5 <i>Water Matrices .....</i>	<i>12</i>
2.5.1 <i>Seawater.....</i>	<i>12</i>
2.5.2 <i>Groundwater .....</i>	<i>13</i>
2.5.3 <i>Mud Volcano and Volcanic Waters.....</i>	<i>13</i>
2.5.4 <i>Landfills – Monitoring wells, storm drains and leachate.....</i>	<i>13</i>
2.5.5 <i>Urban Water - River &amp; Lake Water.....</i>	<i>14</i>
<b>3. Materials and Methods .....</b>	<b>14</b>
3.1 <i>Materials - Chemicals, Reference Materials, Standards and Equipment .....</i>	<i>14</i>
3.2 <i>About the Samples .....</i>	<i>16</i>
3.3 <i>Method - Sample Preparation and Using the prepFAST-system .....</i>	<i>17</i>
3.4 <i>The Instrument – Tuning, Calibration and Analysis .....</i>	<i>18</i>
3.5 <i>Testing the Method .....</i>	<i>19</i>
3.6 <i>Data Analysis and Calculations .....</i>	<i>20</i>
3.7 <i>Accounting for Use of Artificial Intelligence.....</i>	<i>21</i>
<b>4. Results and discussion.....</b>	<b>21</b>
4.1 <i>Addressing the Research Criteria - Method Validation .....</i>	<i>21</i>
4.1.1 <i>The Sensitivity of the Method.....</i>	<i>21</i>
4.1.2 <i>Recovery Rates .....</i>	<i>23</i>

4.1.3 Column Lifetime .....	24
4.1.4 The Precision of the Method.....	26
4.1.5 Accuracy in the Method.....	27
<i>4.2 Addressing the Research Question - <math>\delta^{11}B</math> and Boron Concentrations in the various matrices</i> .....	28
4.2.1 Mud Volcano and Volcanic Waters .....	30
4.2.2 Seawater .....	31
4.2.3 Landfill Leachate, Monitoring Wells and Storm Drains .....	32
4.2.4 Groundwater .....	35
4.2.5 River and Lake Water .....	36
<i>4.7 Method Development</i> .....	36
<b>5. Conclusion.....</b>	<b>38</b>
<b>6. Further Work .....</b>	<b>38</b>
<b>7. References .....</b>	<b>39</b>
<b>Appendix A - Data Manipulation and Calculations.....</b>	<b>44</b>
<b>Appendix B – Raw Data.....</b>	<b>49</b>
<b>Appendix C – Precision of The Method .....</b>	<b>56</b>
<b>Appendix D – Column Lifetime Raw Data .....</b>	<b>57</b>
<b>Appendix E – pH Effect on Recovery.....</b>	<b>58</b>

# 1. Introduction

## 1.1 The Objective of This Thesis

There exists a relatively large mass difference between  $^{11}\text{B}$  and  $^{10}\text{B}$  of 10%, which facilitates isotope fractionation in geochemical processes (Marschall & Foster, 2018). The development of a method to analyze boron isotopes can be valuable in tracking pollution sources, pH reconstruction in seawater, helping the nuclear industry in reactor safety systems, and to study geological processes. The aim of this thesis is to apply and optimize an already existing method in a paper by de la Vega et al. 2020 on various aqueous matrices with different boron concentrations. The authors of this paper measured the ratio of the two stable boron isotopes ( $^{11}\text{B}/^{10}\text{B}$ ) in coral, seawater and carbonate sample (de la Vega et al., 2020). Chromatographic separation was achieved through the ESI prepFAST Automated Inline Dilution System, coupled to Amberlite IRA743, a boron-specific ion exchange resin. The isotope ratio was quantified using a multicollector inductively coupled plasma mass spectrometer (MC-ICP-MS). The same was done here using specifically Thermo Scientific Neptune Plus, and atomic total boron concentrations were also measured using High-Resolution ICP-MS (Thermo Scientific Element2/XR), as well as the signal intensity from the multicollector. The aim of this thesis aligns with MetroPOEM's broader goal of developing SI-traceable methods for stable isotope ratio measurements.

The water matrices analyzed here included 9 categories, Groundwater, Landfill Leachate, Mud Volcano, Seawater, Urban Water – River, Urban Water – Storm Drain from Landfills, Lake Water, and Volcanic Water from different geographic regions. Laboratory work was conducted at the Institute for Energy Technology (IFE) in Lillestrøm, Norway, in collaboration with the Norwegian University of Life Sciences (NMBU). A total of 299 unique samples were analyzed using the method, totalling 372 measurements. 84 measurements were measured as part of this thesis and 288 samples were later analyzed at the IFE stable isotope laboratory using the final method as a part of the laboratory's daily activities. A problem encountered when studying boron isotopes is fractionation of boron during the chromatographic separation and in the ICP-instrument. In addition, boron is considered an adhesive element leading to memory effects. Addressing these issues requires high recovery rates (near 100%) and effective washing procedures when using the ICP-MS-instrument.

## 1.2 Research Questions and Research Criteria

**Research Question:** Will the measured boron concentrations and  $\delta^{11}\text{B}$ -values align with the theoretical values for each of the aqueous matrices?

**Research Criteria:** To validate the method's precision and accuracy, 4 criteria were set. If these criteria are fulfilled it can be said that the application of the method to the aqueous matrices is successful.

**Criteria 1:** The LOD of the atomic concentration using the method will be below 3 ng/mL.

**Criteria 2:** The standard deviation (SD) between replicate measurements'  $\delta$ -values should not be greater than 5 permille (‰).

**Criteria 3:** The Amberlite IRA743 resin will effectively separate boron from aqueous matrices, with quantitative recovery of 95-105% for all samples, avoiding fractionation.

**Criteria 4:** The measured  $\delta^{11}\text{B}$ -value of the certified reference material ERM-123 should show a standard deviation of less than 1‰, compared its theoretical  $\delta^{11}\text{B}$ -value of  $-0.40 \pm 0.60\text{‰}$ .

## 2. Theory

### 2.1 Boron Isotopes, Fractionation and Applications

Boron is a light element with an atomic number of 5 and an atomic mass of 10.811 amu. It has two stable isotopes,  $^{10}\text{B}$  (19.9%) and  $^{11}\text{B}$  (80.1%). The isotopes react similarly chemically, although their masses are different, with  $^{10}\text{B}$  having a mass of 10.0129369 amu and  $^{11}\text{B}$  a mass of 11.0093052 amu. This mass difference of 10% leads to isotope fractionation in nature, which occurs through two main processes, equilibrium isotope exchange reactions and kinetic processes (Hoefs, 2015). The main difference being that in equilibrium fractionation, the isotope ratio changes until it reaches equilibrium, whereas kinetic processes are unidirectional (Tiwari, et al., 2015). Because of this its isotope ratios serve as a useful geochemical tracer (Marschall & Foster, 2018). Boron has a wide range of industrial applications, for instance, due to its use in detergents, boron isotopes can be valuable for tracing contamination sources in the environment.

Understanding the distribution of boron is also important for interpreting concentrations and the fractionation processes that affect boron isotope ratios. Boron isotope ratios are typically reported as  $\delta$ -values, which represent the difference in isotopic composition relative to a specific standard representing the published isotopic composition, expressed in parts per thousand (‰). The  $\delta$ -value can also be understood as the permille difference of the heavier isotope amount in a sample in comparison to the standard.  $\delta$ -values are used to analyze fractionation patterns in nature, and are calculated using the following equation.

$$1) \quad \delta^{11}\text{B} (\text{‰}) = \left( \frac{\left(\frac{^{11}\text{B}}{^{10}\text{B}}\right)_{\text{Sample}}}{\left(\frac{^{11}\text{B}}{^{10}\text{B}}\right)_{\text{NIST 951a}}} - 1 \right) \times 1000$$

In Equation 1, the measured boron ratio in a sample, together with a measured boron standard ratio, NIST<sub>951a</sub> is used. The commonly used standard for  $\delta^{11}\text{B}$ -values is NIST boric acid SRM 951a, referred to in this thesis as NIST<sub>951a</sub>. This standard has an isotope ratio of 4.04558 (Hoefs, 2015), giving  $^{10}\text{B}$  (19.9%) and  $^{11}\text{B}$  (80.1%), which is same as the given theoretical value of boron isotope concentrations in nature. Because NIST<sub>951</sub> is chosen as the standard used in the calculation of boron isotope  $\delta^{11}\text{B}$ -values, its own  $\delta^{11}\text{B}$ -value is defined as 0 by Equation 1.

In aqueous solutions, boron exists in equilibrium between boric acid ( $B(OH)_3$ ) and borate anions, where the most common is tetrahydroxyborate ( $[B(OH)_4]^-$ ), an acid-base equilibrium that is pH-dependent, with a  $pK_a$  of 9.24. In alkaline solutions higher than pH 9.24, borate predominates, while in acidic conditions, or below pH 9.24, boric acid is dominant. The equilibrium can be represented as:



It is seen in equation 2 that the coordination of boron is trigonal planar for boric acid, and tetrahedral for borate. Boric acid contains more  $^{11}B$  than  $^{10}B$  relative to the borate anion due to  $^{11}B$  favoring the shorter B-O bonds found in the trigonal planar coordination (Kowalski et al., 2013). Because of this isotope fractionation occurs in Equation 2 and it dependent on the pH of the solution. This has been shown in several natural systems, such as the accumulation of the borate ion in the carbonate skeleton of marine calcifiers (Banks & Rae, 2020). The boron isotopic composition in marine calcium carbonates can be used as a tracer for past pH and because of this it can aid in reconstruction of past  $CO_2$  levels in the atmosphere (Saldi et al., 2018; Hoefs, 2015).

Boron in the aqueous environment originate from a variation of sources, and is it not possible to point to a single boron source, as there exists a natural flux of boron in nature, referred to as the boron cycle. The boron cycle is referred to in a paper by Schlesinger and Vengosh from 2016 as having been in a steady state for over 1 000 000 years (Schlesinger & Vengosh, 2016). There are also many industrial emissions of boron, and while the boron cycle is in a steady state, the antropogenic flux is dynamic (Schelsinger & Vengosh, 2016). For example, sodium perborate (Figure 1) is a bleaching agent, which is added to detergents and cleaning products, and is removed by release into waters (Barth, 1998).

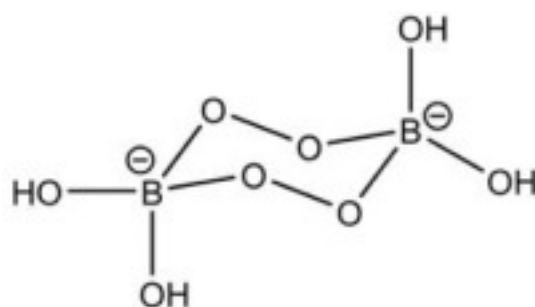


**Figure 1** – Illustration of the perborate anion (Darvell, 2018).

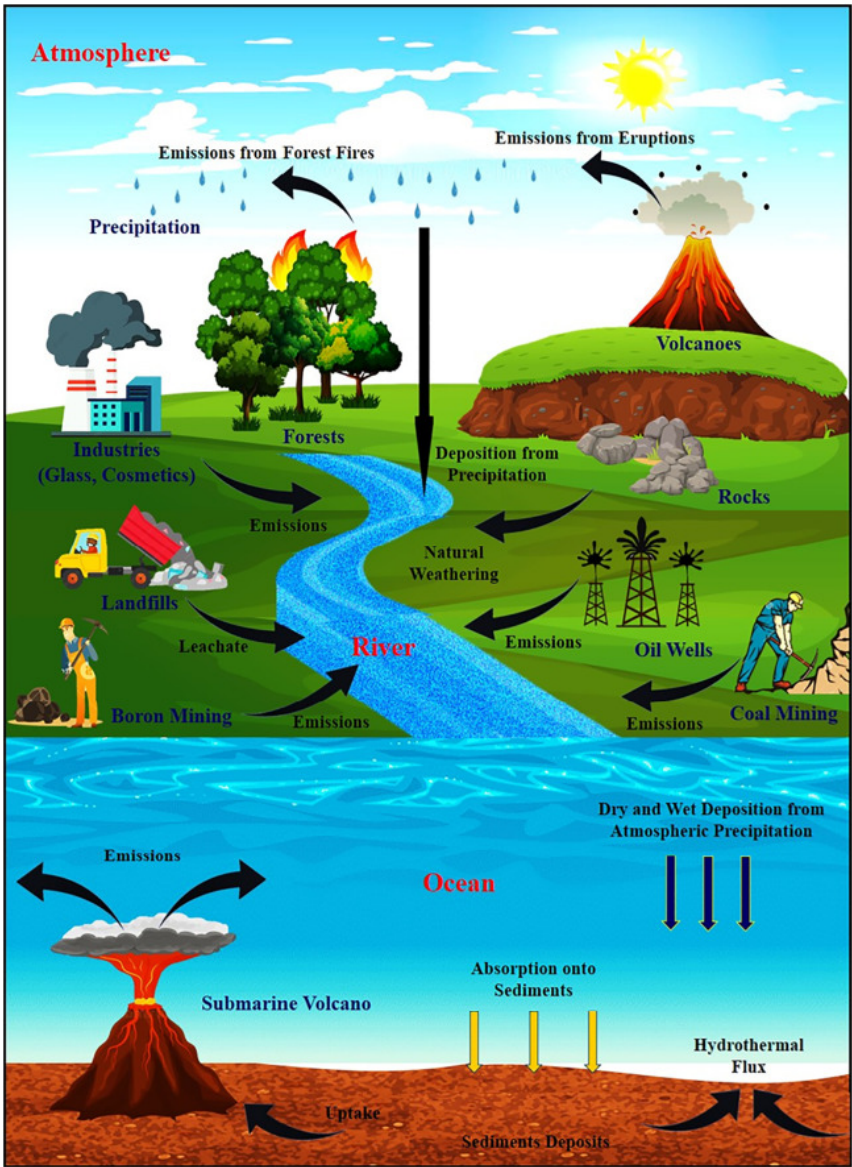
Figure 1 shows the structure of perborate anion, and when released into the waters the  $\delta$ -value of sodium perborate show a distinct signature in contaminated water of 0 to 10 ‰, which can be used to trace the source of anthropogenic pollution (Sankoh, 2022). Significant boron sources also include coal mining and combustion, the oil industry and mining and processing of boron ores (Schlesinger & Vengosh, 2016).

To compare boron concentrations and  $\delta^{11}\text{B}$ -values across various matrices, it is useful to reference literature values. Table 1 summarizes the predicted boron concentrations (in mg/L) and  $\delta^{11}\text{B}$ -values for different aqueous matrices. This table will serve as a reference throughout this thesis to evaluate whether the obtained data align with existing literature, addressing Research Question 1, whether the measured boron concentrations and  $\delta^{11}\text{B}$ -values will align with the theoretical values for each of the aqueous matrices. It should be noted, however, that the reference values for mud volcanoes and rivers are based on specific localities and may not be representative of regional or global variations. For Landfill Leachate, comparisons can be more complex due to the variable boron concentrations and  $\delta^{11}\text{B}$ -values, which are influenced by the composition of the waste in the landfill. However, theoretical concentration values for Landfill Leachate, along with other matrices, are provided in Table 1.

**Table 1** – Concentration of boron in mg/L and  $\delta\text{B}^{11}$ -value for various matrices.

Matrix	Concentration (mg/L)	$\delta\text{B}^{11}$ (‰)	Reference
Meteorite	0.3-1.4	-50-40	Lecuyer, 2018
Upper continental crust	17	-5-(-15)	Lecuyer, 2018
Mud Volcano	100 - 868	15	Kopf & Deyhle, 2002
Volcanic waters	17.5-82.1	-10-0	Millot et al., 2020
Soil	1-1000		Bolan, 2023
Seawater	4.5	39.61	Foster, Lecuyer & Marschall 2018; Foster, Lecuyer & Marschall 2016
Groundwater	<0.3-100	0-50	Marschall & Foster, 2018
Rivers	0.001-0.2 (mostly <0.02).	-10.6-47.3 (mostly 2-20)	Mao et al., 2019
Freshwater lake	0.0003-0.044	-4.4-59	Lecuyer, 2018

Table 1 shows the theoretical boron concentration (mg/L)  $\delta$ -values in various geological matrices. As shown in Table 1, boron is typically found in concentrations ranging from 1 to 1000 mg/L in soil. Boron is essential for plants, and its primary entry pathway is through soil in its soluble form, such as boric acid. While boron is mainly found in solution in soil, it is also present in minerals, clay, organic matter, and biomass (Arunkumar, 2018). Boron concentrations in rocks vary widely depending on the rock type and location (Arunkumar, 2018). In rocks, boron commonly occurs in the form of oxygenated borate minerals, with borax ( $\text{Na}_2\text{B}_4\text{O}_7 \cdot 10 \text{H}_2\text{O}$  or  $\text{Na}_2[\text{B}_4\text{O}_5(\text{OH})_4] \cdot 8 \text{H}_2\text{O}$ ) being one of the most well-known examples of borate minerals. Figure 2 summarizes the boron flux or cycle in nature.



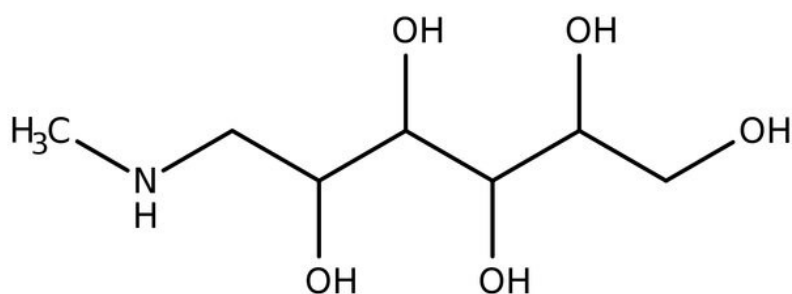
**Figure 2** – Illustration of the natural flux of boron in nature (Bolan et al., 2023).

Figure 2 shows that boron is released into water bodies from a wide range of sources, including weathering from rocks, oil wells and fossil fuel combustions, and industrial and mining emissions. Volcanic eruptions also release boron into the atmosphere. Boron leaves the atmosphere through meteoric precipitation (rain/snow) as well as via dry deposition. Waterways ultimately transport the boron into the sea, which itself is also affected by rainwater, submarine volcanoes and hydrothermal flux.

## 2.2 Automated Chromatography with prepFAST and IRA743

The isotope ratio data is measured through analysis by mass spectrometry. For boron, MC-ICP-MS has become increasingly common, however, TIMS can also be used, as well as SIMS for solid samples (Marschall & Foster, 2018). To accurately measure boron isotope ratios in aqueous matrices, the sample must first be separated from its matrix to avoid interferences, which is achieved using ion exchange chromatography. Potential interferences include beryllium hydride ( ${}^9\text{Be}^1\text{H}$ ), or doubly charged neon ( ${}^{20}\text{Ne}^{++}$ ) on mass 10, or spread of the mass 12 peak from  ${}^{12}\text{C}$  overlapping with the  ${}^{11}\text{B}$  peak when there is high organic content or low boron content. The interferences will be most significant when there is a low boron concentration, such as in lake waters or rivers.

In this thesis, the ESI prepFAST Automated Inline Dilution System was used with Amberlite IRA743, a boron-specific resin. The N-methyl D-glucamine (NMDG) functional group in IRA743 selectively binds borate ions ( $\text{B}(\text{OH})_4^-$ ) (Marschall & Foster, 2018), allowing boron to be isolated from complex aqueous matrices (Figure 3). This automated system has advantages over manual methods, increasing efficiency and reproducibility in laboratory settings, in addition to lowering the uncertainty of the analysis.



**Figure 3** – The N-methyl-D-glucamine (NMDG) functional group, can form complexes to the borate ion  $\text{B}(\text{OH})_4^-$ .

However, boron is removed from solution by forming a complex with NMDG, and not solely ion exchange, and because of this boric acid can also bind. The reactions that can form are seen in Figure 4.

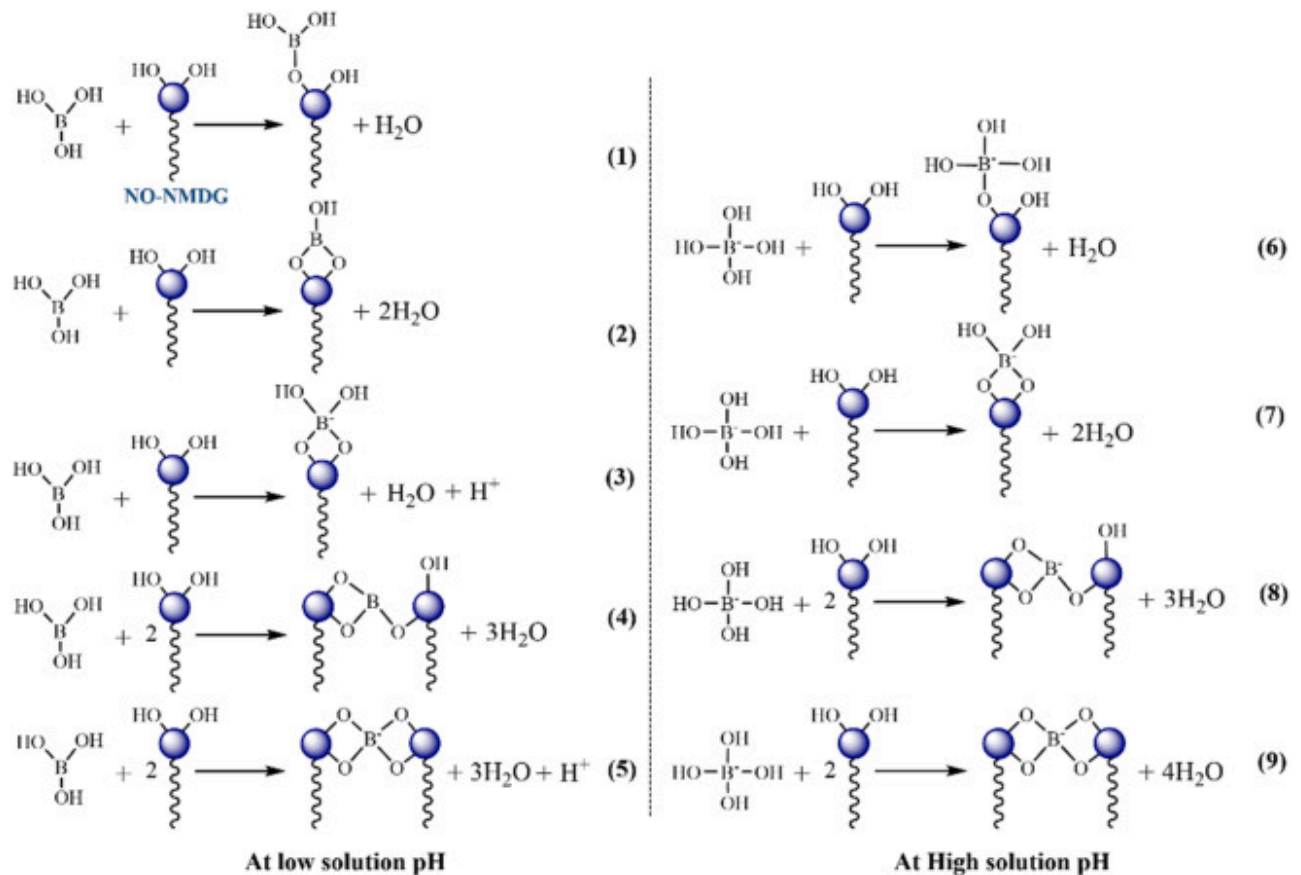


**Figure 4** – Complexation between boron and a NO-NMDG functional group (Bai et al., 2021).

It is seen that the complexation between the resin and boric acid at low pH in reaction 3 and 5 yield protons in solution, and because of this the equilibrium shifts to the left (Bai et al., 2021). The borate anion will elute more readily as the complex is less stable than that for boric acid (Landsman et al., 2021). When the pH is between 4-8.30 the NMDG functional group is positively charged, and there is electrostatic attraction stabilizing the complex formed between the borate anion and the resin, this increases recovery (Bai et al., 2021).

The method used in this thesis, involves buffering the sample with ammonium acetate to convert boric acid into the borate anion (see Figure 3). However, many studies advocate for using a basic pH, preferably 8, as most of the boron will be found as the borate anion, which will bind more easily to the column, as well as forming a less stable complex with the NMDG

functional group of the resin (Bai et al., 2021; Landsman et al., 2021; Wei et al., 2014). The less stable complex makes the boron release and elute from the column more easily when an acid is used as an eluant, reacting the borate anion back to boric acid (Figure 5).

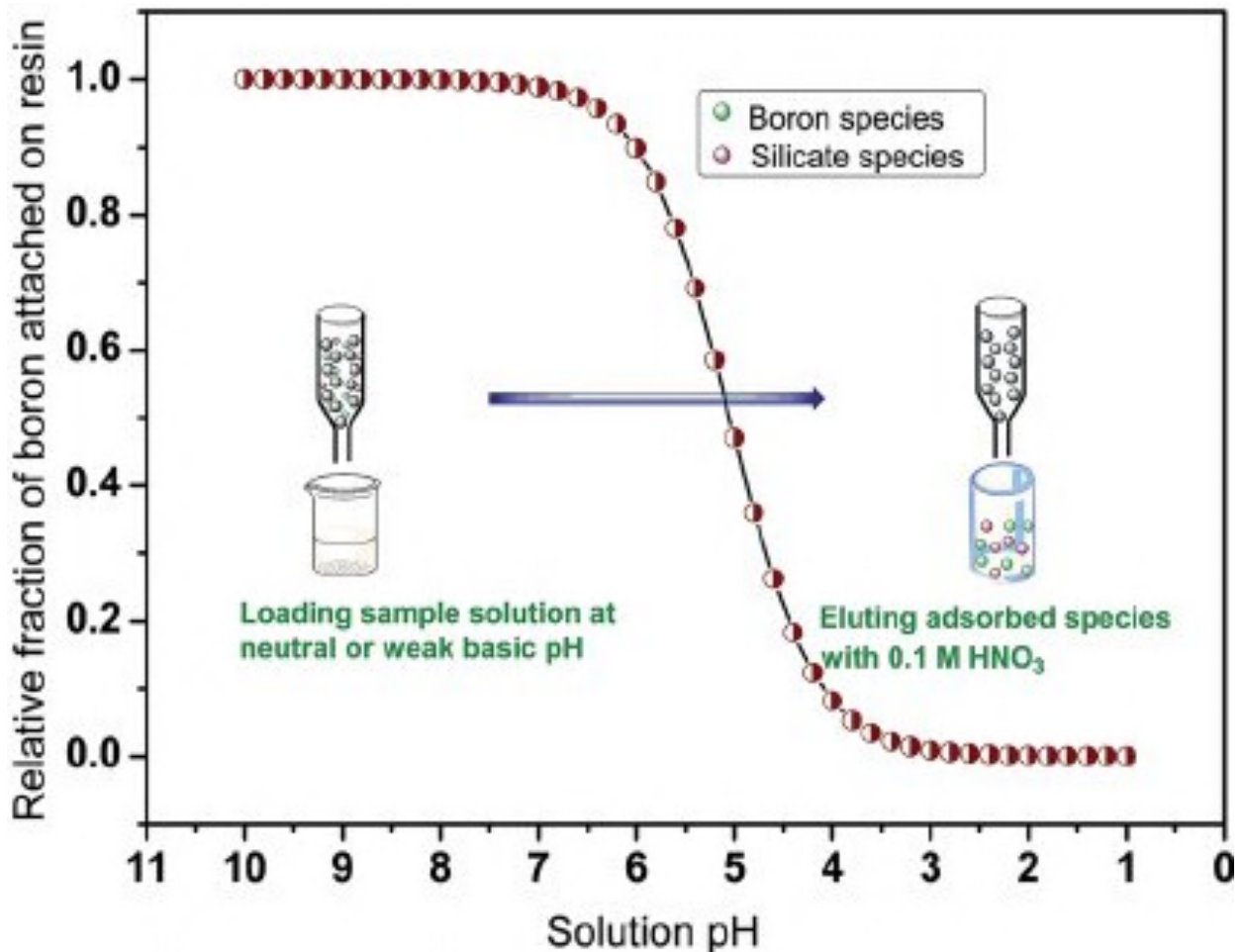


**Figure 5** - Adsorption to the IRA743 resin as a function of the pH of the solution (Wei et al., 2014).

Figure 5 shows that at a pH of 8.0, 100% of the boron should be attached to the IRA743 anion resin. The boron is subsequently eluted using 0.1 mol/L nitric acid (HNO<sub>3</sub>), which shifts the equilibrium back to boric acid, allowing it to be collected for isotope analysis. However, in the paper from 2020 by de la Vega et al., the authors claim that the optimal pH is 5.5, which is what is used here in this thesis. The paper by Bai et al., does however, claim that if the pH is between 4-8.30 the recovery will be higher than below or above this pH-range, which supports the use of a pH of 5.5. According to the literature, at low pH, there will be little

borate which can bind to the resin as most is found as boric acid, and at a very high pH above 8.30, hydroxides ( $\text{OH}^-$ ) will compete for binding the column, decreasing recovery rates.

### **2.3 Inductively Coupled Plasma Mass Spectrometry**

Throughout this thesis, the Neptun instrument will be referred to as the MC-ICP-MS and the Element2/XR as the HR-ICP-MS. Boron measurements were performed using both HR-ICP-MS for concentration analysis and MC-ICP-MS for isotope analysis. However, atomic concentrations of boron were also measured using the signal intensity of  $^{11}\text{B}$  in the sample related to the intensity of a reference material with known concentration (NIST SRM 951a) used for calibration of the isotope ratio to the  $\delta$ -scale.

ICP-MS was developed in the 1980s, and has become a widely used instrument capable of measuring concentrations from ppq to ppm (Jensen, 2020). ICP-MS comprises two components: the ICP and the MS. The ICP ionizes the sample using an inductively coupled plasma, while the MS separates ions by mass-to-charge ratio. The sample is introduced via a peristaltic pump and nebulizer, creating an aerosol that passes through a spray chamber to remove large droplets. Smaller droplets enter a plasma torch where argon gas is ionized to form a plasma (Wilschefski & Baxter, 2019).

The ICP operates at atmospheric pressure, and the MS at a vacuum, connected by an interface with cones to prevent clogging and contamination (Neufeld, 2019). The MS separates ions by mass-to-charge ratio. Instruments like the Neptune and Element2/XR use metal Faraday cups for high signals and electron multipliers (EM) for lower signals, which amplify the ion signal to be measured (Wilschefski & Baxter, 2019). Using an electrostatic analyzer (ESA) before the magnet, kinetic energies can be filtered, giving more narrow peaks (Schönbachler, 2018). High resolution mass spectrometers also have adjustable entrance and exit slits before and after the mass analyzer, allowing for a mass resolving power of over 10 000 (Marshall et al., 2013).

Boron is considered an adhesive or “sticky” element, and has a well-known problem with memory effects. Thus, it requires a long wash-out time, or the utilization of “non-standard” washing solutions. One such method involves using a sodium fluoride (NaF) solution (He et al., 2019), to form volatile  $\text{BF}_x$  complexes which are easier to wash out of the sample

introduction system. To avoid putting the probe directly from a sample to a washing solution, a pre-wash solution can be used to minimize cross-contamination.

Another challenge in measuring boron is the space-charge effect, which occurs when the ion beam enters the mass spectrometer. Heavier elements (e.g. Na and Cl in seawater) tend to concentrate in the center of the ion beam, while lighter elements, such as boron, are pushed to the edges because the ions all have the same charge, repelling each other. As boron is a light element with high relative mass difference, this effect is exacerbated, and can make it more difficult to correctly measure boron. It also leads to isotope fractionation, where more  $^{10}\text{B}$  relative to  $^{11}\text{B}$  will be pushed to the side of the ion beam and interact with the cones. This both creates buildup of the lighter boron isotope on the cones which can lead to an increased background, and also depressed  $^{10}\text{B}$  sample signal relative to  $^{11}\text{B}$ . However, by successfully separating boron using ion exchange chromatography, this issue can be mitigated, reducing the impact of space-charge effects. However, there may still be isotopic fractionation arising from the inlet system as the lighter  $^{10}\text{B}$  will tend to migrate towards the sides of the ion beam. This instrumental isotopic fractionation is a function of the inlet system and can be accounted for by determination of the degree of fractionation by analysis of standards with known isotopic ratios before and after the sample.

All samples were measured using standard-sample bracketing, a technique where a standard is measured first, followed by the sample, and then another standard is measured at the end. Although this method extends the duration of the analysis, it plays a critical role in ensuring the accuracy of the measurements. By calculating the  $\delta$ -value using the two standards, any drift in the instrument during the measurement process is corrected continuously throughout the analysis, thereby improving the reliability of the data.

## **2.4 Measurements and Uncertainty**

When measuring isotope data on the MC-ICP-MS there will be blocks and cycles of measurements, for which a standard deviation is calculated for each isotope concentration and ratio. If it is necessary to correct for the presence of a signal blank by subtracting the mean isotope concentration value from the sample, the uncertainty increases. There also lies uncertainty arising from sample preparation and the chromatography step with prepFAST. The standard deviation of multiple operations using multiplication and division is calculated according to this formula.

$$3) \sigma_{\text{TOT}} = x_{\text{TOT}} \cdot \sqrt{\left[ \frac{\sigma_1^2}{x_1} \right] + \left[ \frac{\sigma_2^2}{x_2} \right]}^1$$

The software already gives the uncertainty in the measurement from the instrument. Thus, the standard deviation calculated within the different matrices in terms of concentration and  $\delta B^{11}$  is calculated as

$$4) s = \sqrt{\frac{\sum_{i=1}^n (x_i - \bar{x})^2}{n-1}}$$

## 2.5 Water Matrices

The water types evaluated in this work include Landfill Leachate, Storm Drain – Landfill, Mud Volcano water, Seawater, Groundwater, Urban Water – River, Lake Water, and Volcanic Water. The different sample categories can be divided into three groups based on their boron concentration: low, medium, and high. The Mud Volcano water, Volcanic Waters, Landfill Leachate, and Seawater are classified as having high boron concentrations, exceeding 1000 ng/mL. Groundwater is categorized as having a medium boron concentration, typically ranging from 300 to 1000 ng/mL. Medium concentration is defined here as a concentration between 200-1000 ng/mL. Finally, Lake Water, and the various Urban Waters (including River, and Storm Drain Landfill) are classified as having low boron concentrations, ranging from 0 to 200 ng/mL.

### 2.5.1 Seawater

Seawater refers to the water from the world's oceans and seas. There are variations in seawater composition, particularly in terms of salinity and concentrations of other species, such as boron (Duxbury et al., 2024). A substantial proportion of the boron in seawater comes from weathering of rocks (Marschall & Foster, 2018). As rocks in the earth's crust weather, boron and other elements are released into rivers, which eventually flow into the oceans, contributing to seawater's boron content, which was seen in Figure 1 depicting the boron cycle. There are also other factors affecting the boron content of the seawater, such as precipitation from the atmosphere, and emissions from the industry and combustion of organic matter. The boron content of seawater is expected to be relatively uniform, with a

---

<sup>1</sup> (Jerome 2023)

$\delta^{11}\text{B}$  value around 39.61‰, and a concentration of approximately 4.5 mg/L, as shown in Table 1. Consequently, seawater is considered to have a high boron concentration relative to other environmental samples and the other aqueous matrices.

#### **2.4.2 Groundwater**

Groundwater is defined as water present underneath the unsaturated (vadose) zone, commonly found in aquifers. Groundwater is significant because it is often used as a source of drinking water. Due to the heterogeneous nature of groundwater, boron sources can vary, including contributions from weathered rocks, soil, the atmosphere via the rain, and leaching from various sources like rain and snowmelt, as well as anthropogenic inputs. These are the same sources affecting the boron content of rivers and oceans, however, groundwaters are separated from each other, and reflects the specific environment in which it is located. Therefore, both boron concentrations and  $\delta^{11}\text{B}$  values can vary significantly, as shown in Table 1, with concentrations reported in the literature ranging from <0.3 to 100 mg/L and  $\delta^{11}\text{B}$  values from 0 to 50‰.

#### **2.5.3 Mud Volcano and Volcanic Waters**

A Mud Volcano erupts mud, water, and gases. These formations occur when fluids and gases accumulate beneath the Earth's surface, eventually erupting and bringing mud to the surface (Hudec, 2023). The boron concentration and  $\delta^{11}\text{B}$  values in mud volcanoes should be interpreted based on this, including boron containing minerals in the mud and water that are transported upward. The Mud Volcano samples measured here comes from Lusi/Sidoarjo, Indonesia. Volcanic Waters, as defined in this thesis, are waters influenced by volcanic activity, specifically from volcanic provinces in Italy. Volcanic activity means that the boron concentration and  $\delta^{11}\text{B}$ -value will be affected by the magma and fluids being transported. Consequently, the boron concentration and  $\delta^{11}\text{B}$  values in volcanic waters are expected to be high, ranging from 100 to 868 mg/L, with a  $\delta^{11}\text{B}$  value of approximately -10-0‰.

#### **2.5.4 Landfills – Monitoring wells, storm drains and leachate**

Landfills contain waste from urban environments, and rainfall can produce landfill leachate from the landfill components. Landfills mitigate this problem by using separate systems for leachate collection and for surface water runoff, however, due to the risk of leachate contamination of local groundwater, they also conduct groundwater monitoring. Boron concentrations and  $\delta^{11}\text{B}$  values can vary between landfills, depending on the specific content

of the landfill. Because of this categorizing landfills based on  $\delta^{11}\text{B}$  values can be useful for tracking the movement of Landfill Leachate.

### 2.5.5 Urban Water - River & Lake Water

Lakes are water inland that can originate from various sources, which also affects their boron content. It is important to interpret boron concentrations and  $\delta^{11}\text{B}$  values in lakes accordingly. Urban Waters, which include rivers, storm drains, tap water, and landfill leachate, are influenced by human activities. As a result, urban waters are often affected by anthropogenic factors such as air pollution, contamination, and sewage. In urban environments, water runoff from buildings, roads, and tunnels can also affect boron contents. Rivers analyzed in this thesis are expected to have relatively low boron concentrations, as rivers receive boron through weathering processes, but due to the continuous flow of water, boron concentrations are generally low. Additionally, with new water inputs constantly entering the river, the concentration of boron is further reduced, preventing accumulation of boron in the river water. As seen in Table 1 rivers can be expected to have a  $\delta$ -value like seawater (40‰ and 39.61‰, respectively) or as low as -10‰, with a range from -10.6-47.3‰. Rivers are like groundwater in their boron  $\delta$ -values, and because of this there will be regional and global variations. Rivers are also primarily constituted of groundwater and meteoric water.

## 3. Materials and Methods

### 3.1 Materials - Chemicals, Reference Materials, Standards and Equipment

This thesis used a variety of chemicals, some requiring dilution. All dilutions were made using ultrapure/Type 1 (18.2 M $\Omega$ -cm) water (Milli-Q H<sub>2</sub>O). The ultrapure water will further be referred to as Milli-Q water in this thesis. Table 2 provides an overview of the chemicals used in this analysis.

**Table 2** – Overview of the chemicals used in this analysis

Chemical/gas	Formula	Concentration	Manufacturer
Ammonium acetate	NH <sub>4</sub> CH <sub>3</sub> CO <sub>2</sub>	4 mol/L	Elemental Scientific (ESI)
Ammonium acetate	NH <sub>4</sub> CH <sub>3</sub> CO <sub>2</sub>	5 mol/L	Sigma-Aldrich
Nitric acid	HNO <sub>3</sub>	65% (w/w), 2 mol/L & 0.5 mol/L	Sigma-Aldrich
Milli-Q water	H <sub>2</sub> O		Merck
Argon	Ar		
Sodium fluoride	NaF		Sigma-Aldrich

The nitric acid (HNO<sub>3</sub>) listed in Table 2 was distilled using sub-boiling distillation in the laboratory prior to use. Sodium fluoride (NaF) originated from a powder which was dissolved using Milli-Q water to the appropriate concentration. The ammonium acetate purchased from ESI was used without dilution, while the Sigma-Aldrich ammonium acetate was diluted to 4 mol/L using Milli-Q water when needed.

Seven certified reference materials (CRMs) were used during the study, as summarized in Table 3. The table also provides  $\delta^{11}\text{B}$ -values,  $^{11}\text{B}/^{10}\text{B}$  ratios, and  $^{10}\text{B}/^{11}\text{B}$  ratios for some of the CRMs.

**Table 3** – Overview of the reference materials and standards used in this analysis. Their  $\delta\text{B}^{11}$ -value and  $\text{B}^{11}/\text{B}^{10}$  as well as  $\text{B}^{10}/\text{B}^{11}$  ratio is also provided.

	Concentration	Manufacturer	$\delta\text{B}^{11}$ (‰)	$\text{B}^{11}/\text{B}^{10}$ ratio	$\text{B}^{10}/\text{B}^{11}$ ratio
<b>Boric acid isotopic standard NIST<sub>951a</sub></b>		NIST			0.2473 ± 0.0002
<b>ERM-AE120</b>		BAM	-20.2 ± 0.6	3.963 ± 0.006	0.25236 ± 0.00033
<b>ERM-AE121</b>		BAM	19.9 ± 0.6	4.127 ± 0.006	0.24233 ± 0.00032
<b>ERM-AE122</b>		BAM	39.7 ± 0.6	4.205 ± 0.006	0.23782 ± 0.00031
<b>ERM-AE123</b>		BAM		4.042 ± 0.006	0.2474 ± 0.0004
<b>IV-ICPMS-71</b>	10 µg/mL B 3% (v/v) HNO <sub>3</sub>	Inorganic Ventures			
<b>Boron ICP standard</b>	1000 mg/L H <sub>3</sub> BO <sub>3</sub> in H <sub>2</sub> O	Sigma-Aldrich			

As seen in table 3, the CRMs provide different certified information. AE120 is only certified for its  $\delta B^{11}$ -value, AE121 and AE122 both for  $\delta B^{11}$  and  $B^{11}/B^{10}$  ratio. AE123 is only certified for its  $B^{11}/^{10}B$  ratio. When using reference materials for  $\delta^{11}B$  corrections, the CRMs AE120, AE121 and AE122 were used. The IV-ICPMS-71 and Boron ICP standard were only used for the HR-ICP-MS. NIST951<sub>a</sub> is boric acid and the ERM-AE120/121/122/123 reference materials are all an aqueous boric acid solution.

All equipment, including 50 mL tubes and prepFAST vials, were PFA-based and boron-free. The washing protocol involved a 24-hour acid bath (10%  $HNO_3$ ), followed by rinsing with Milli-Q five times. The equipment was then air-dried in the fume hood.

### 3.2 About the Samples

In total, the dataset comprises 299 unique samples over 9 categories of aqueous matrices with varying boron concentrations, totalling 372 measurements. 84 measurements were analyzed personally and 288 samples were later analyzed at the IFE stable isotope laboratory using the final method. All samples were collected by IFE and prepared at their stable isotope laboratory. Among the samples analyzed later, some only included boron concentration measurements, while a few also contained  $\delta^{11}B$ -values. Recovery data and certified reference materials used is only available for the 84 measurements that were personally analyzed.

These categories include groundwater samples, consisting of 53 deep groundwater samples collected from monitoring wells at three landfills in Norway (Øras, Horisont, and Sirkula), and shallow groundwater samples collected from wells or boreholes on Zakynthos Island, Greece. These two categories have been merged together to represent the Groundwater category. Lake water is represented by 64 samples from various Norwegian lakes. Two samples from the Lusi Mud Volcano in Indonesia constitute the Mud Volcano category. Seawater includes 2 unique samples, one from the North Sea, and one from the Mediterranean, sampled off Zakynthos Island, Greece, with a total of 10 measurements. Landfill Leachate consists of 15 samples. Urban Water comprises 48 river water samples from Norway, corresponding to 53 measurements, along with 107 samples and measurements from storm drains near landfills. Finally, volcanic water is represented by 7 samples collected in Italy, corresponding to 7 measurements.

### 3.3 Method - Sample Preparation and Using the prepFAST-system

The samples were filtered and diluted with Milli-Q water to reach a volume of 1.5 mL, depending on the initial concentration, the aim was to reach a target concentration of 500 ng/mL in the final solution after addition of acid and buffer, representing a medium concentration of boron. The reason for dilution being that too high concentrations of boron would overload the column, and potentially induce isotope fractionation, and memory effects resulting in a high background. Additionally, would too high boron concentrations might potentially wear out the cones by clogging them over time. Following the dilution, 0.5 mL of 2 mol/L HNO<sub>3</sub> and 2 mL of 4 mol/L ammonium acetate were added, bringing the total volume to 4 mL. The prepared samples were pipetted into prepFAST PFA vials and placed in a custom-designed rack compatible with the prepFAST system. If samples were not immediately analyzed, they were sealed with PFA caps to prevent potential contamination from the air and reducing the possibility of isotopic fractionation due to evaporation, as <sup>10</sup>B will evaporate more readily than <sup>11</sup>B, due to its lighter mass.

The prepFAST system was used for the automated ion exchange chromatography step. As shown in Figure 5, the filtered water sample (1.5 mL) was mixed with 2 mL of 4 mol/L ammonium acetate and 0.5 mL of 2 mol/L HNO<sub>3</sub>. This mixture was then introduced into prepFAST vials and loaded onto the prepFAST system, which was set up with a separation column containing Amberlite IRA743, a boron-specific ion exchange resin. The system processed the samples by preferentially binding boron and washing away other matrix elements, allowing boron to be isolated and eluted (Figure 6).

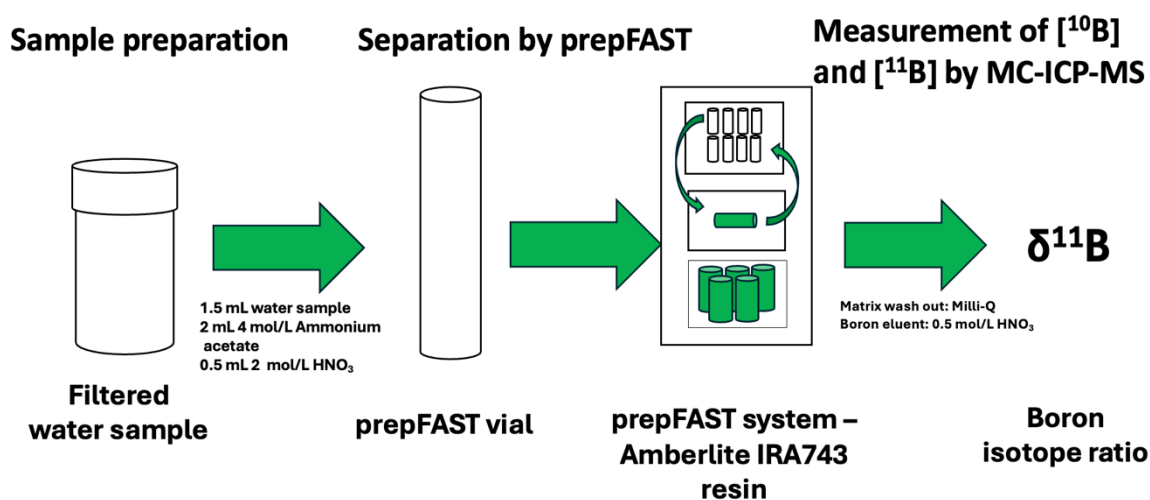


Figure 6– Diagram illustrating the method employed.

The program used for the prepFAST can be seen in table 6. The vials with the eluted boron are analyzed by MC-ICP-MS. The program used for the prepFAST system is outlined in Table 4.

**Table 4** – Program used for prepFAST.

	<b>Cycles</b>	<b>Destination of reagent</b>	<b>Reagent fill volume (μL)</b>	<b>Reagent</b>
<b>Cleaning of column</b>	1	Waste	2000	HNO <sub>3</sub>
<b>Conditioning of column</b>	1	Waste	2000	Milli-Q
<b>Sample load</b>	1 or 3	Waste	1000	Sample
<b>Washing of matrix</b>	1	Waste	1000	Milli-Q
<b>Elute</b>	1	Destination 1	500	HNO <sub>3</sub>

The column is first cleansed using 2 mL 0.5 mol/L HNO<sub>3</sub>, and conditioned with 2 mL Milli-Q water to a pH of 5, where the amine group on the NMDG functional group will be positively charged. Once the sample was loaded onto the column, the matrix components were removed through a washing step with Milli-Q water. Boron was then eluted by washing the column with 500 μL 0.5 mol/L HNO<sub>3</sub>, converting borate ions back into boric acid. Most of the boron is eluted at 300 μL, and because of this the method can be adjusted to 300 μL (de la Vega et al., 2020). This allowed for the collection of boron in new prepFAST vials, which were subsequently analyzed using the MC-ICP-MS. It is possible to adjust the number of cycles of sample loading, allowing for the introduction of more sample volume, and thus more boron from low-concentration samples. However, this also increases the concentration of any boron present in the reagents.

### **3.4 The Instrument – Tuning, Calibration and Analysis**

On the ICP-MS, it was important to tune the instrument, especially if any modifications have been made to the instrument parameters. This is because the instrument needs to be calibrated, stabilized, optimized in terms of sensitivity. The tuning is saved in a tuning file. Regardless, tuning was checked every time when using the instrument. A tuning solution of NIST<sub>951a</sub> 100 ng/mL was used in this thesis, corresponding to a concentration of 17.5 ng/mL boron. It was

made from another diluted NIST951a solution, made from the original NIST<sub>951a</sub> reference material. The many steps increase the uncertainty of the concentration of the tuning standard. The intensity is made as high as possible manually by adjusting factors such as lenses and torch position corresponding to the highest intensity signal possible. The Faraday cup positions were also calibrated to make sure the cups correspond to the desired mass to be analyzed, the cups H3 (<sup>11</sup>B) and L3 (<sup>10</sup>B) were used. This information was saved in a cup calibration file, which was reused unless adjustments were necessary.

After tuning, the samples were analyzed manually by means of standard-sample bracketing, and a thorough washing routine between samples and standards. The ICP-MS analysis had to be operated manually as there was no autosampler working, hence this step was time-consuming, and limited the number of samples that could be analyzed during the time frame of the thesis.

The washing procedure between samples involved a brief rinse in a prewash solution of 2% HNO<sub>3</sub>, followed by 1.5 minutes in a NaF solution, and finally 2.5 minutes in 2% HNO<sub>3</sub>. To improve efficiency, the probe was not washed between the blank and a sample or standard. During analysis, the signal intensity of the sample, blank, or standard was monitored during a 1-minute take-up time before the actual measurement started.

When analyzing concentration data, it is important to make a calibration curve. This is done by measuring standards with known concentration and making a calibration curve. The equation of the calibration curve is used to calculate the concentration of the sample. This way the intensity measured by the instrument can be converted to a concentration. For the isotope analysis on the MC-ICP-MS it was used using the tuning solution of a 100 ng/mL NIST<sub>951a</sub> standard.

### **3.5 Testing the Method**

Initially, the method was tested using the HR-ICP-MS with IV-ICPMS-71A from Inorganic Ventures as the boron standard. Sodium chloride (NaCl) was added to mimic the composition of seawater. Various ratios of boron to salts were experimented with during these preliminary tests. NaCl was added at varying concentrations, which gave unrealistically high salt concentrations, much higher than for seawater. Because of this, to preserve the instrument, these samples had to be diluted, with increased the uncertainty of the results. The original

solution not undergoing chromatographic separation, the elute of the chromatography and the wash solution were all kept in their respective vials. The raw solution, elute and wash solution were measured on the HR-ICP-MS. The raw solutions contained 5.0 ng/mL boron, the sodium (Na) 93.1, 1503, 2190.3, 4658.5 and 6301.3 ng/mL Na, and the chlorine (Cl) 4, 950.4, 1480.6, 3407.4 and 4897.8 ng/mL Cl. After this, the salt concentration was kept constant at 2100 ng/mL, with a varying boron concentration of 20, 30, 50, 70, 90, 100, 120, 140 and 150 ng/mL boron. Finally, 11 samples were tested using the method by de la Vega et al., from 2020, with concentrations of NIST<sub>951a</sub> 0-10 ng/mL boron, no salt added. Following these trials, the method was then applied to the MC-ICP-MS for isotope analysis using water samples where the boron concentrations were already known. Subsequently, the method was used to analyze additional samples using this procedure.

To investigate the effect of pH on the recovery rates, the pH of samples was measured after the prepFAST separation process. Seawater from the North Sea was used as a sample, and various ratios of HNO<sub>3</sub>, sample, Milli-Q water, and ammonium acetate were tested (see Appendix E).

The lifetime of the ion exchange resin Amberlite IRA743 was also tested on the MC-ICP-MS. A diluted seawater sample containing 33 ng/mL boron was analyzed repeatedly on the same IRA743 column for 144 samples. Every 10<sup>th</sup> sample in addition to blanks were analyzed. It was previously unknown how effective the regeneration of the column is using this method and at what point the recovery rates decline increasing the possibility of induced isotopic fractionation.

### **3.6 Data Analysis and Calculations**

All data analysis was performed using Microsoft Excel, with detailed calculation examples provided in Appendix A. All data analyzed throughout this work, including preliminary testing, was included in the results. The last three analyses conducted in April represent samples analyzed using the final optimized method, and include alternating sample and instrumental blanks, as well as all the set of all four ERM-AE reference materials (AE120, AE121, AE122 and AE123), of which three are used for calibration of the  $\delta$ -scale and the fourth as an “unknown”. The first isotope analysis (23/01/2024) contains no blank, and only two reference materials (AE122 and AE123). The analysis on 01/03/2024 contains two reference materials (NIST<sub>951a</sub> and AE122) and one blank only, because of this bias could not

calculated for this analysis. The analysis on 05/03/2024 only AE123 was used, so there was no  $\delta$ -correction, but bias could be calculated, and there were alternating sample blanks. On 20/03/2024 three reference materials were used (AE120, AE121 and AE122), but not AE123, and four blanks were used.

It is seen that different reference materials were used in some analyses, which means that some of the  $\delta^{11}\text{B}$ -values are corrected differently, because of this the precision cannot be evaluated between replicates in the method. In addition, the first analysis from 10/01/2023 did not use a sample blank correction, meaning that this analysis cannot be compared to all the other analyses, in which are corrected using a sample blank. The final three sequences can however be compared, because the same reference materials and calibration protocols were used.

The LOD and LOQ were calculated taking the standard deviation between the blanks times 3 and 10 respectively. It was calculated using the three final analyses, which included alternating blanks and four CRMs (AE120-123), representative of the optimized method. See Appendix A for specifications about the calculations.

### **3.7 Accounting for Use of Artificial Intelligence**

Artificial Intelligence (AI) has been used in this thesis for language polishing, and as an aid in understanding the data. The AI program used was OpenAI's ChatGTP (ChatGTP-4).

## **4. Results and discussion**

### **4.1 Addressing the Research Criteria - Method Validation**

#### **4.1.1 The Sensitivity of the Method**

The method was validated according to its sensitivity, recovery, precision, and accuracy. One of the analyses (20/01/2024) was removed from the results as all the samples were saturated, making the ICP-MS data unreliable. The sensitivity of the method, as determined by the LOD and LOQ, was found to be 1.4 ng/mL and 4.5 ng/mL, respectively. This meets Research Criteria 1, which states that the LOD must be below 3 ng/mL. A LOD of 1.4 ng/mL makes it possible to measure the concentration of most aqueous matrices, although lake water typically can have concentrations lower than 1.0 ng/mL. Achieving a LOD lower than this can be

challenging, as boron often has a high background due to its presence in the atmosphere, as well as its adhesive properties leading to memory effects, resulting in a higher LOD compared to other elements. The average blank concentration was found to be 2.3 ng/mL across all blanks used in all the analyses, which is significant. Because of this the reagents were checked for atomic boron concentration using the HR-ICP-MS (Table 5).

**Table 5 – B concentration (ng/mL) in reagents used in the method**

<b>Reagent</b>	<b>B concentration (ng/mL)</b>
<b>Ammonium Acetate, 5 mol/L, Sigma-Aldrich</b>	3.9
<b>Ammonium Acetate, 4 mol/L, ESI</b>	11.6
<b>HNO<sub>3</sub> 2M</b>	2.5
<b>MQ-H<sub>2</sub>O</b>	< 0.2

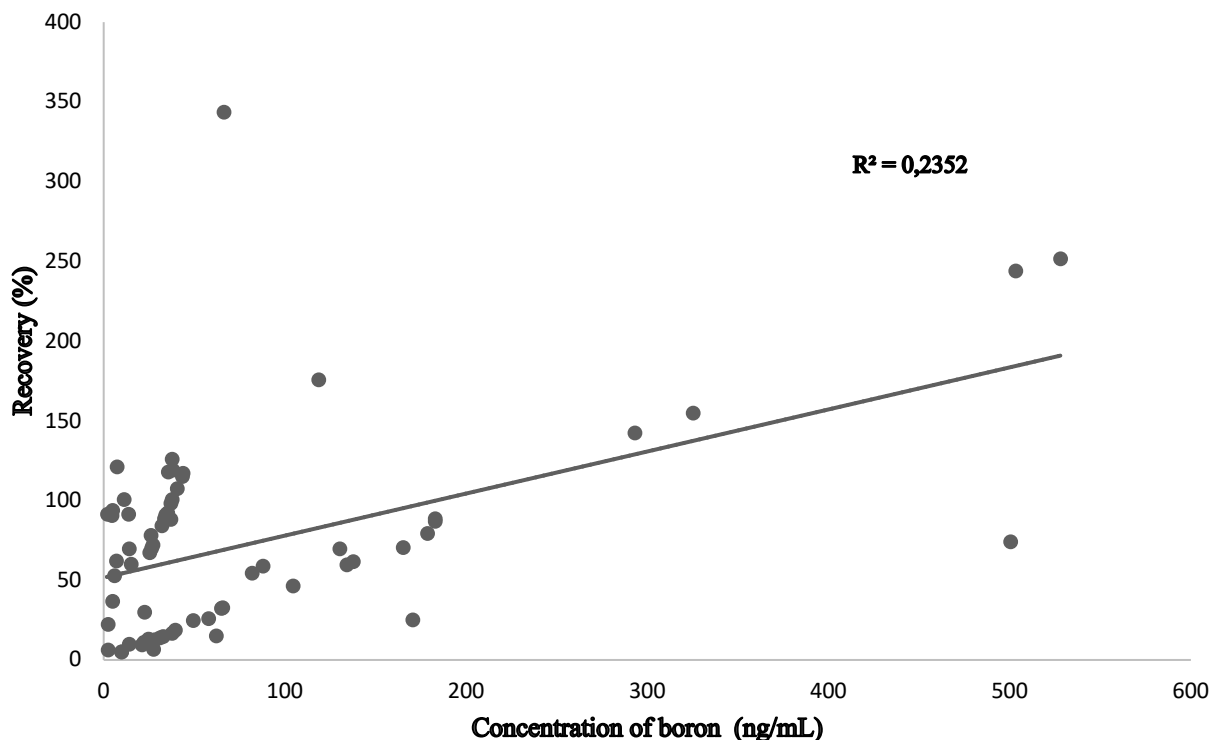
As seen in Table 5 the ammonium acetate from Sigma-Aldrich contains 3.9 ng/mL boron. This was the buffer that was used in the beginning of this work, and because this was found, a new ammonium acetate reagent of 4 mol/L advertised as boron free from ESI was used. The buffer from ESI turned out to contain 11.6 ng/mL boron, containing even more boron than the initially used buffer. Because of this, the ammonium acetate from Sigma-Aldrich continued to be used. It was also found 2.5 ng/mL boron in the HNO<sub>3</sub>, despite distillation, and the MQ-H<sub>2</sub>O contained very little boron (<0.2 ng/mL).

When using the ammonium acetate from ESI, the background would be increased by 6.1 ng/mL. On the other hand, when using the one from Sigma-Aldrich the background was increased with 2.3 ng/mL. This is significant, because 2.3 ng/mL was the average concentration of boron in all the blanks used in the analyses. These values are both combined with the boron found in the nitric acid which contained 2.5 ng/mL boron. The main limiting factor in establishing a low LOD using ICP-MS is often how clean the method is. The boron contaminated reagents used here significantly impacted the LOD and LOQ of this method, and further studies should try to use a different buffer containing as little boron as possible, which will likely result in a lower LOD, which might enable the detection of boron in all potential low boron concentration water samples, like lake water. The buffer does not necessarily need to be ammonium acetate, it can be any base, and some papers use NaOH. However, the effects of different bases on the regeneration of the IRA resin and possible complications from a high cation load should be considered, including higher pressures

potentially required for the pumps in an automated system or the need for reverse wash step not necessary when using ammonium.

#### 4.1.2 Recovery Rates

In addition to sensitivity, recovery rates were evaluated across a range of boron concentrations. Although it is known that higher recovery rates are more easily achieved at higher concentrations, regression was used to give an overview of the recovery values as a function of concentrations (Figure 7).



preferably a pH of 8, and as seen when measuring the pH, the samples' pH is 5.5. At this pH most of the boron will be found as boric acid, because the pKa-value of boric acid is 9.24. It is harder for boric acid to bind to the resin, and when bound its complex is more stable, making it harder to elute than boron found as the borate anion. This can possibly account for the lower recovery rates.

However, making the sample basic with a base to pH = 8 is not what is seen in the literature of papers where IRA743 is used in the method, and many studies advocate for using a pH of 5.5, and have 100 % recovery rates, like in de la Vega et al., 2020. A study by Bin Darwish, Kochkodan and Hilal from 2015 looked at the effect of pH on the IRA 743 and found that the recovery was best at pH = 8, and insufficient at 5 or lower (Bin Darwish, Kochkodan & Hilal, 2015). It is uncertain why de la Vega et al. got recovery rates of 100 %.

Erring on the side of increased recovery through high pH for increased binding might also lead to fractionation. Leftover boron on the column from a previous sample, and memory effects can lead to artificially high recovery rates. However, if that is the case the 100% recovery rate found will not be stable across all samples, which is found in de la Vega et al. 2020. In this work, some samples showed recovery rates of 100%, however, this was not consistent within the analysis, which indicate that excess boron was left on the column or there were memory effects. Boron contamination also leads to higher recovery rates, but because the sample and instrumental blanks' concentration is subtracted from the measured concentration, this does not affect the calculated recovery rates.

#### **4.1.3 Column Lifetime**

It was also speculated whether the recovery rates would decline over time, as the column becomes worn-out. There is no literature on this, although de la Vega proposes that this is 60 samples, if the samples contain 20 ng boron on a carbonate matrix. The lifetime of the ion exchange resin Amberlite IRA743 was also tested on the MC-ICP-MS. A diluted seawater sample containing 33 ng/mL boron was analyzed repeatedly on the same IRA743 column for 144 samples using 1.0 mL of the sample, meaning that there is 33 ng boron per cycle or sample. The raw data can be found in appendix D, and the results are shown graphically in Figure 8.

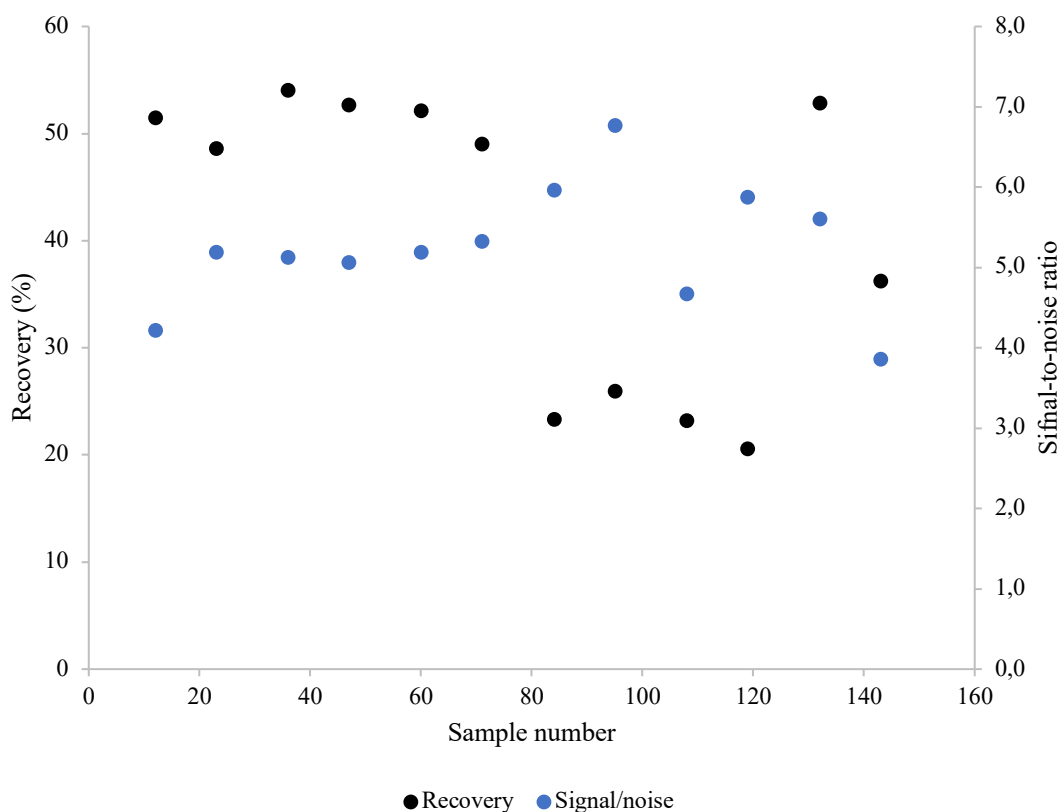


**Figure 8** – Scatter plot showing % recovery and signal-noise ratio against numbers of samples run through the column.

Stable recovery rates > 50% are obtained for the first 72 separations, with subsequent separation showing a significant drop in boron recovery to approximately 38 % (Figure 6). It is also seen that the signal-to-noise ratio declines after number of samples run through the column. Most samples had much higher concentrations, and in varying degrees. In total this would be 2541 ng boron assuming there was no boron in the blanks. If there were no boron in the blanks, 2541 ng boron would be a good indication of the number where the column needs to be changed. However, because this number assumes that there is no boron in the blanks, this number is probably higher.

Interestingly, the recovery rate is not 100 %, although it is stable. This indicates that the recovery rates are not high enough to meet the criteria of recovery rates between 95-105%, although the content eluted will be stable across the samples. Again, by trying to increase the pH, speculatively, the recovery rate will be higher, and by changing the column when the 2541 ng limit has been reached, high stable recovery rates with potentially less fractionation can be obtained.

#### 4.1.4 The Precision of the Method

The precision of the method was evaluated by calculating the standard deviation of the  $\delta$ -values for replicates corrected using the same reference materials. A relative standard deviation (RSD) could not be used because the  $\delta$ -values are in permille, and this would make the deviations artificially high. Table 6 summarizes the standard deviation values for 13 sample replicates including 6 CRMs and 7 environmental samples.

**Table 6** – Precision of the method, represented by the standard deviation of  $\delta$ -values for replicates corrected using the same reference materials.

n	ID	Replicates	Sample type	$\delta$ -correction	SD
1	2023-074-002	2	Groundwater	AE120, AE121, AE122	2,52
2	2023-109-042	3	Seawater	AE120, AE121, AE122	6,48
3	2023-126-011	2	Landfill Leachate	AE120, AE121, AE122	1,40
4	2023-126-012	2	Landfill Leachate	AE120, AE121, AE122	3,49
5	2023-135-020	2	Landfill Leachate	AE120, AE121, AE122	4,87
6	2023-136-001	4	Seawater	AE120, AE121, AE122	12,75
7	2023-138-004	2	Landfill Leachate	AE120, AE121, AE122	1,13
8	AE120	4	Reference material	AE120, AE121, AE122	2,21
9	AE121	4	Reference material	AE120, AE121, AE122	3,74
10	AE122	4	Reference material	AE120, AE121, AE122	2,25
11	AE122 2	2	Reference material	No correction	2,87
12	AE123	2	Reference material	AE120, AE121, AE122	10,42
13	NIST951a	3	Reference material	No correction	2,62

Most replicates had standard deviations below 5 %, with the exceptions of the seawater sample 2023-136-001 and the CRM AE123, which revealed higher standard deviations. The  $\delta$ -values within the replicates can be seen in Appendix C. Because of this Research Criteria 2 was not met, which stated that all the replicate groups should have standard deviations less than 5%.

The seawater sample from the North Sea (2023-136-001) had  $\delta$ -values of 38.84 ‰, 43.10‰, 41.29‰, and 66.34‰ over four independent analyses, with corresponding recovery rates of

78%, 17%, 62%, and 13%, respectively. The theoretical  $\delta$ -value for seawater is 39.61‰, and the closest observed value (38.84‰) was associated with the highest recovery rate of 78%, the second closest value (41.29‰) belonging to the second highest recovery rate of 62%. Similarly, the CRM AE123 showed a high standard deviation of 10.42‰, with replicates yielding  $\delta$ -values of -12.49‰ and 2.25‰, although the theoretical  $\delta$ -value is  $-0.40 \pm 0.60$ . The corresponding recovery rates for these replicates were 13% and 69%.

As seen in Appendix C, the  $\delta$ -values generally show a standard deviation below 5‰ for most replicate groups, which is surprising given that the recovery rates are quite variable. However, few replicates were measured, and many cannot be used because they are not corrected using the same CRMs. It follows that when the recovery rates are unstable and low, leading to fractionation, the precision of the method will also be low, leading to consequential errors in the precision.

#### 4.1.5 Accuracy in the Method

AE123 has a certified boron isotope ratio of  $4.042 \pm 0.006$  and certified  $\delta$ -value of  $-0.40 \pm 0.6$ . The results of the measured isotope ratios for AE123 are summarized in Table 7, which also shows the corresponding recovery rates and standard deviations from the  $\delta$ -value of AE123. Just like the RSD cannot be calculated due to the  $\delta$ -values being in permille, this cannot be done for accuracy either. Because of this the standard deviation from this true value is used instead.

**Table 7** – Table showing the accuracy in the analysis as reflected by the standard deviation of the expected  $^{11}\text{B}/^{10}\text{B}$  isotopic composition for the certified reference material ERM-AE123.

n	ID	Date analyzed	RM used for $\delta^{11}\text{B}$ correction	Recovery	$\delta^{11}\text{B}$	Expected $\delta^{11}\text{B}$	Uncertainty	SD
1	AE123	23/01/2024	No correction	93	-6,67	-0,4	0,6	4,4
2	AE123	05/04/2024	AE120, AE121, AE122	13	12,49	-0,4	0,6	8,5
3	AE123	17/04/2024	AE120, AE121, AE122	69	2,25	-0,4	0,6	1,8
4	AE123	23/01/2024	No correction	94	-1,01	-0,4	0,6	0,4
5	AE123	12/03/2024	No correction	60	4,87	-0,4	0,6	3,7
6	AE123	26/04/2024	AE120, AE121, AE122	1	-50,21	-0,4	0,6	35

The observed  $\delta$ -values range from -50.21 to 12.49, with recovery rates varying between 1% and 94%. The calculated standard deviations ranged from 0.4-35, which is not acceptable. The lowest standard deviation was 0.40 at a recovery of 94 %. The second lowest standard deviation (1.8) was observed for a  $\delta$ -value of 2.25 at a recovery rate of 69%. AE123 was measured as  $\delta^{11}\text{B}$  of -50.21 at 26/04/2024, which gives a standard deviation of 35, and is far from the theoretical value of -0.40. Because of this the Research Criteria 4, claiming that the standard deviation from AE123's theoretical  $\delta^{11}\text{B}$ -value should be less than 1‰ is not met here. One possible explanation for this might be substantial fractionation, due to the low recovery rates in some analyses.

#### 4.2 Addressing the Research Question - $\delta^{11}\text{B}$ and Boron Concentrations in the various matrices

The raw data for  $\delta^{11}\text{B}$  values and boron concentrations are provided in Appendix B. Table 8 summarizes the range of boron concentrations (ng/mL) and  $\delta^{11}\text{B}$  values (‰) with corresponding standard deviations for Volcanic Waters, Mud Volcano, Seawater, Landfill Leachate, Groundwater, Urban Water – River, and Urban Water – Storm Drain Landfill. Theoretical boron concentrations and  $\delta^{11}\text{B}$  values for selected matrices are also included.

**Table 8** –  $\delta^{11}\text{B}$  values (‰) and boron concentrations (ng/mL) across different matrices using the method.

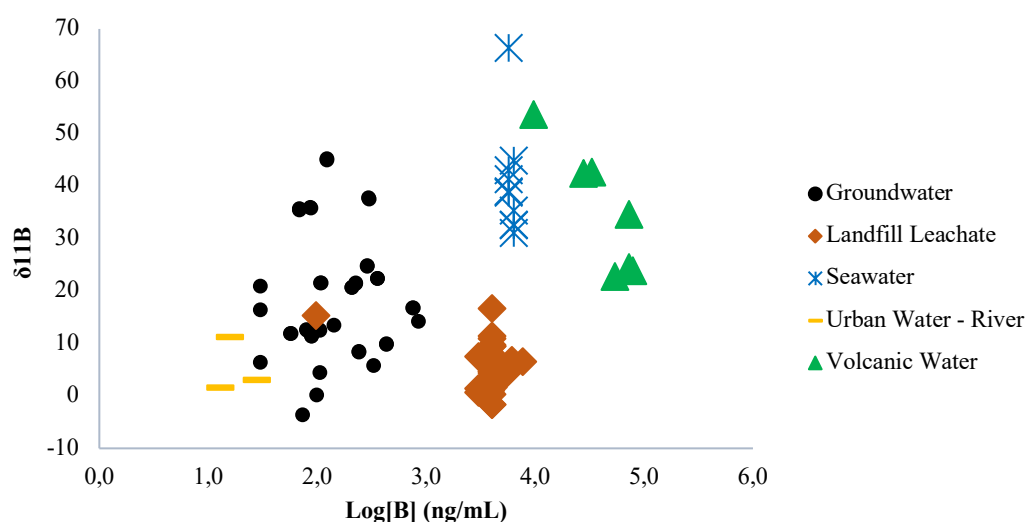
Matrix	$\delta^{11}\text{B}$ (‰)	Boron concentration (ng/mL)	Theoretical $\delta^{11}\text{B}$ (‰)	Theoretical boron concentration (ng/mL)
Mud Volcano		200-102 000 (n = 2)	15	100 000 – 868 000
Volcanic Waters	23-54 (n = 7)	9737-79 468 (n = 7)	-10-0	17 500-82 100
Seawater	31-66 (n = 10)	5750-6413 (n = 2)	39.61	4500
Landfill Leachate	-2-17 (n = 26)	3041-4125 (n = 8)		2000-4000
Groundwater	-4-45 (n = 41)	30-844 (n = 49)	0-50	300-100 000
Urban Water - River	1-11 (n = 3)	3-39 (n = 48)	-10.6-47.3	1.0-200
Urban Water – Storm Drain Landfill		2-121 (n = 107)		
Lake Water		1.4-58 (n = 24)	-4.4-59	0.3-44

Table 8 shows boron concentration and  $\delta^{11}\text{B}$ -values ranges across the different water matrices. The measured concentrations of boron aligns with the theoretical values for most of the matrices except for Seawater, where the measured values are somewhat higher than the

global mean concentration. The table is arranged from highest concentration of boron on the top of the table, and lowest at the bottom. The two Mud Volcano samples exhibited concentrations ranging from 200 to 102 000 ng/mL. The  $\delta$ -values for these two samples could not be determined as the all the samples in this analysis were too concentrated leading to saturation of the faraday cups, making the  $\delta$ -values unreliable. Volcanic Waters showed concentration ranging from 9.7 to 79 mg/L boron, and a  $\delta$ -value ranging from 23 to 54%. For Seawater elevated concentrations of 5.8 to 6.4 mg/L were observed, and a  $\delta$ -value of 31-66%.

Landfill Leachate had lower boron concentrations of 3.0 to 4.1 mg/L boron and a  $\delta$ -value of -2 to 17%. A theoretical value for Landfill Leachate's  $\delta$ -value could not be found.

Groundwater was found from 13 – 844 ng/mL boron, and -4-45 %, making the  $\delta$ -values very different. Urban Water – River samples had a much lower concentration at 3 to 39 ng/mL, with 1-11 %. Storm drain Landfill showed a concentration from 2-121 ng/mL, and no  $\delta$ -values were measured, nor was it possible to find a theoretical values for the concentration or  $\delta$ . Tap Water only contained 4 ng/mL boron. All Lake water samples, with concentrations below the LOD of 1.4 ng/mL, could not be measured using this method. However, for the ones that could be detected, a concentration of 1.4-58 ng/mL was found. The overall relationship between boron concentration and  $\delta^{11}\text{B}$  values was visualized using a scatter plot, where  $\delta^{11}\text{B}$  is plotted against the logarithm of boron concentration (ng/mL) using base of 10 (Figure 9).



**Figure 9** -  $\delta^{11}\text{B}_{\text{NIST951a}}$  plotted against  $\log_{10}$  boron concentration ng/mL.

From Figure 9, samples from the same matrix tend to cluster together. It is important to note that the x-axis uses a logarithmic scale, emphasizing differences in concentration between matrices. Like in Table 8 Volcanic Waters display high concentrations of boron (over 1.0 mg/L), however, the  $\delta$ -values are somewhat arying, although all  $\delta$ -values are positive. Landfill Leachate samples also show high boron concentrations, with much lower  $\delta^{11}\text{B}$ -values, ranging from -2-17‰.

Seawater samples form a distinct concentration cluster, because only two seawater samples were measured between 5750-6413 ng/mL, and the  $\delta$ -values range from 31-66 ‰, also corresponding to a high boron concentratino. Groundwater samples are more dispersed in their  $\delta^{11}\text{B}$  values, and also vary more in concentration than the other categories, from low concentration (below 200 ng/mL boron) to medium concentration (200-1000 ng/mL boron). The three data points for Urban Water – River shows a low boron concentration below 200 ng/mL and a low  $\delta$ -value below 20‰.

#### **4.2.1 Mud Volcano and Volcanic Waters**

Mud Volcano and Volcanic Waters did exhibit the highest concentrations of boron of all categories. The Mud Volcano Lusi in Indonesia, could not have its  $\delta$ -value measured, because of saturation in the analysis without subsequent dilution, and because of this fractionation cannot be compared to the litterature. However, the Mud Volcano concentration was 200-102 000 ng/mL which is within the theoretical concentration range of 100 000–868 000 ng/mL. In a paper written by Kopf & Deyhle from 2002, it is stated that the  $\delta^{11}\text{B}$  value of Mud Volcano fluids are generally lower than that of seawater, around 15 ‰, where seawater is about 39.6‰. The authors hypothesize Mud Volcanoes to be a significant contributor to backflux into the hydrosphere from the lithosphere (Kopf & Deyhle, 2002). The measured  $\delta$ -value for Mud Volcano found here was 11.04 and 3.78‰, however, for the Mud Volcano sample with 102 000 ng/mL boron, the sample was saturated. This suggests that the Mud Volcano  $\delta$ -values found here are lower than seawater's  $\delta$ -value of 39.6 ‰, aligning with the literature, however, the results shown here must be interpreted with caution due to the saturation of the sample, meaning that the ICP-MS could not reliably measure the sample's concentrations.

The Volcanic Waters show a lower concentration of 9737 to 79 468 ng/mL boron, and is defined as water influenced by volcanic activities sampled in central Italy. Specifically, the

Volcanic Waters from Italy's concentrations were, 79468 ng/mL  $\delta^{11}\text{B}$  of 23.86‰, 72962 ng/mL and  $\delta^{11}\text{B}$  of 24.46‰, 72669 ng/mL and  $\delta^{11}\text{B}$  of 34.59, 54136 ng/mL and  $\delta^{11}\text{B}$  of 22.84‰, 33016 ng/mL and  $\delta^{11}\text{B}$  of 42.75‰, 27848 ng/mL and  $\delta^{11}\text{B}$  of 42.47‰ and 9737 ng/mL and  $\delta^{11}\text{B}$  of 53.57‰. These concentrations of boron align with the literature, but not the  $\delta$ -values, which were predicted to be about -10 to 0 ‰. The values found here align more with seawater  $\delta$ -values of about 39.61 ‰. In a study about geothermal waters from Millot et al., 2012, boron concentrations were found to be 17.5 and 82.1 mg/L, which is what is found here. However, the authors found isotopic compositions negative ranging from -6.7 to 1.9‰, claiming this to be a characteristic  $\delta$ -value of water-rock interaction with magmatic rocks and no seawater input (Millot et al., 2012). Conversely, in a study by Rivas et al., from 2024, heavier  $\delta^{11}\text{B}$ -values can be attributed to interaction with rocks that are isotopically heavy on  $\delta^{11}\text{B}$ , mixed with seawater, or fractionation of a geothermal fluid due to pH, where boric acid under low pH conditions, is isotopically heavier (Rivas et al., 2024).

#### 4.2.2 Seawater

The theoretical  $\delta$ -value of seawater is 39.61‰, and the concentration 4500 ng/mL. The  $\delta$ -value is found within the range found here, however, the concentration from the North Sea and Mediterranean is higher than 4500 ng/mL. According to Foster et al., 2010, the Mediterranean Sea has been reported to have the following  $\delta$ -values in 7 different studies, 37.70-40.30‰, with varying depths from 0-150 m, the North Sea being measured as 40.30‰. The study reports to correlation with depth, salinity or temperature of the seawater, and the overall mean of this study being 39.61 ‰, which is regarded as the theoretical  $\delta$ -value of seawater (Foster et al., 2010). Regarding the concentration, a paper by Farhat et al., from 2013, states that the concentration of boron in seawater can range from 500-9600 ng/mL, and is dependent on the geographical location of the seawater, although the mean is 4500 ng/mL (Farhat et al., 2013). de la Vega et al., 2020 got a  $\delta^{11}\text{B}$ -value of  $39.50 \pm 0.06$ ‰ in seawater, which indicate little to no fractionation using a similar method. Even though the authors used a pH of 5.5, although they got recovery rates of 100%.

Here the seawater sample was measured as 35.38‰, 38.84‰, 32.53‰, 66.34‰. 41.29‰, 31.08‰, 43.10‰ and 44.91‰, comprising the range 32.53 to 66.34‰, with a mean value of  $41.68 \pm 11.11$ , excluding the value of 66.34‰, this range now becomes 32.53 to 44.91‰, which is closer to the theoretical value of 39.1‰. When 66.34‰ was measured, the recovery was 13%, which might have led to substantial fractionation. The measurement with

$\delta^{11}\text{B}=66.34\text{‰}$  appears to be more unreliable than the other measurements, but it is included here for transparency in the data, and to demonstrate the limitations of this method associated with variable recovery.

The best recovery rate obtained for seawater is 78%, which gave a  $\delta$ -value of 38.84‰, which is the closest value to the theoretical value. The other recovery rates are 344%, 67%, 62%, 10%, 17% and 15%, suggesting the possibility of substantial isotopic fractionation and unreliable results. This again shows how important the recovery is when it comes to accurate measurement of the true  $\delta^{11}\text{B}$ -values of samples.

#### 4.2.3 Landfill Leachate, Monitoring Wells and Storm Drains

Landfills Leachate occurs when it rains over a landfill and the water leaches into the ground through the waste layers. A well-managed landfill will have a cover layer and drainage systems to reduce the amount of water infiltration into the waste, but even in the best-managed landfills there is always some water infiltration and leachate production. The results here showed that the Landfill Leachate contained 3041 to 4125 ng/mL boron, with  $\delta$ -values ranging from 7.8 to 15.4‰. Again, the  $\delta$ -value of sodium perborate contaminated water show a distinct signature of 0 to 10 ‰, which can be used to trace the source of anthropogenic pollution (Sankoh, 2022), which is worth noticing, as the  $\delta$ -values found here, seem to align with these values. The theoretical boron concentration is 2000-4000 ng/mL, however, it was not possible to find a theoretical  $\delta^{11}\text{B}$ -value for landfill leachate. A total of 26 measurements of the  $\delta$ -values for landfill leachate were performed, with multiple replicates. The concentration measurements were done using 8 samples. The summarized data, including  $\delta^{11}\text{B}$ -values and concentrations are presented in Table 9.

**Table 9** – The concentration (ng/mL) and  $\delta^{11}\text{B}$  in various landfill leachate samples from different sites

ID	Type	Site	Concentration (ng/mL)	$\delta^{11}\text{B}$
2023-060-009	Landfill leachate	Sirkula	4000	9,41
2023-061-012	Landfill leachate	Øras 2	4000	9,44
2023-074-002	Landfill leachate	IRMAT	4000	9,72

2023-116-001	Landfill leachate	Vestnes renovasjon	4000	8,95
2023-126-011	Landfill leachate	Øras 1	4000	7,84
2023-126-012	Landfill leachate	Øras 2	4000	9,52
2023-135-007	Landfill observation well	Horisont Miljøpark	98	15,37
2023-135-020	Landfill leachate	Horisont Miljøpark	3041	7,55
2023-138-003	Landfill leachate, treated	Esva	6138	8,32
2023-138-004	Landfill leachate	Esva	5467	11,37
2023-144-004	Landfill leachate	IRMAT	7683	9,08

Table 9 shows a relatively homogenous fractionation signature, with the concentrations primarily between 3041 and 4000 ng/mL. An outlier with a  $\delta$ -value of 15.37‰ is found at the concentration of 98 ng/mL. The range of values observed are summarized graphically in Figure 10.

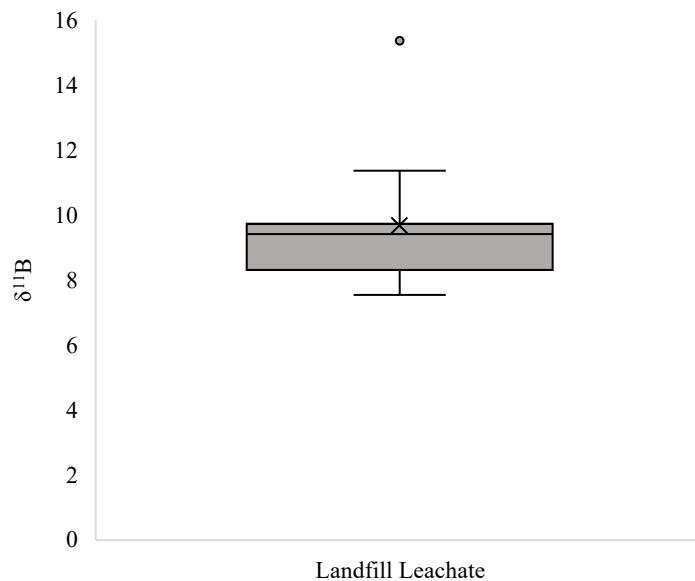


**Figure 10** – Box plot showing the distribution of the  $\delta$ -values in Landfill Leachate measured here.

The box plot shows a narrow range of  $\delta$ -values, with the maximum and minimum values close to the interquartile range. The outlier ( $\delta$ -value of 15.37‰) is seen clearly in this plot, as this is outside the outer limit given the interquartile range. The range excluding the replicates was 7.55 to 15.37‰, and excluding the outlier, 7.55 to 11.37‰. Despite relatively consistent values, poor recovery rates make the data unreliable. Additionally, no theoretical  $\delta$ -value exists for comparison.

The Storm Drains from the landfills showed concentrations ranging from 2-121 ng/mL, and the monitoring wells 216-13 ng/mL. The average boron concentration for Groundwater Monitoring Well, Landfill Leachate and Storm Drain Landfill are shown in Figure 11, where the concentration is logarithmic with a base of 10.

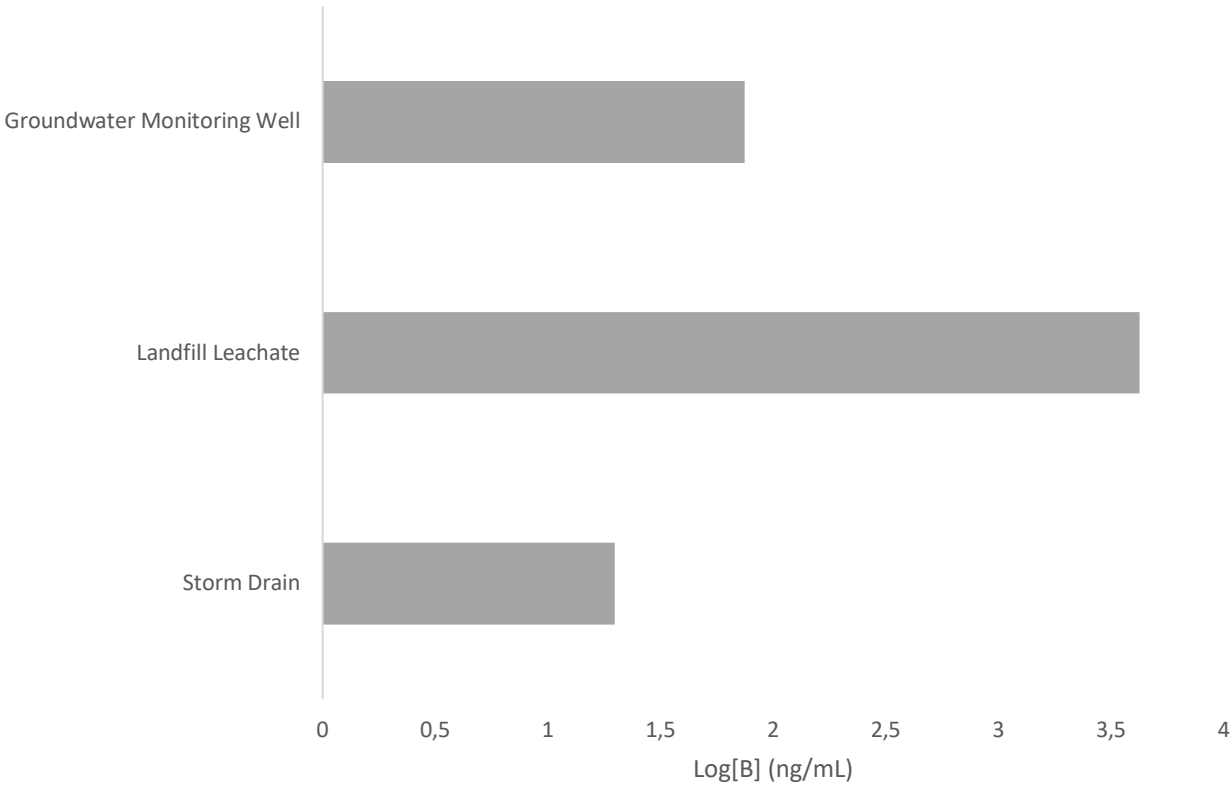


**Figure 11** – Average boron concentration in logarithmic plot, for groundwater monitoring well, landfill leachate and storm drain.

Figure 11 shows that the Landfill Lachate has the highest average boron concentration of 4221 ng/mL boron. This means that there are elevated boron levels here, coming from contamination from the landfill. Landfill Leachate is considered to have high concentrations of boron, as defined here as boron concentrations higher than 1000 ng/mL boron.

Groundwater Monitoring Wells showed the second highest concentration of boron, ranging from 13-216 ng/mL with an average of 75 ng/mL boron, which is defined as a low boron concentration below 200 ng/mL. The theoretical concentration of boron in groundwater is 300 to 100 000 ng/mL, indicating that this groundwater has not been contaminated. However, it is important to remember that boron concentrations in groundwater vary widely, making this hard to interpret. The lowest boron concentration was found in the Storm Drain Landfill category, with a concentration of 20 ng/mL with no measured  $\delta$ -value.

#### **4.2.4 Groundwater**

Groundwater exhibited a wide range of  $\delta^{11}\text{B}$  values from -4 to 45‰ and boron concentrations between 30 and 844 ng/mL. These values align with the theoretical  $\delta^{11}\text{B}$  range of 0 to 50‰ and theoretical boron concentrations of 300 to 100 000 ng/mL. The broad variability can be attributed to the diverse sources contributing to groundwater composition, as well as the independent nature of groundwaters.

Here groundwater was defined as samples from groundwater monitoring wells in Norway and boreholes, and wells on the Zakynthos island in Greece. Shallow groundwater showed a wider range of boron concentrations, from 2 to 844 ng/mL, with  $\delta^{11}\text{B}$  values ranging from 5.76 to 45.30‰. It is important to keep in mind that the shallow groundwater samples were from Greece, and groundwaters vary widely depending on the location. According to a paper by Dotsika et al. from 2006, groundwater samples in Greece, show much higher boron concentration compared to other European countries. In Europe, groundwater concentration of boron higher than 1000 ng/mL is above regulatory limits, which is found in many samples from Greece by Dotsika et al. in 2006, which the authors attributed to thermal waters (Dotsika et al., 2006). This is also what is shown here, although the Dotsika study was conducted in Northern Greece, and samples reported in this work are from the Zakynthos island is located in Southern Greece. Groundwater from the monitoring wells in Norway, on the other hand, displayed boron concentrations between 4.4 and 216 ng/mL, with  $\delta^{11}\text{B}$  values spanning from -

3.6 to 21‰. This shows that the boron concentration in the measured groundwaters in Norway is lower than in Greece.

#### **4.2.5 River and Lake Water**

Of the lake water samples, 40 samples had boron concentrations below the LOD of 1.4 ng/mL. Among the 22 lake samples above the LOD, boron concentrations ranged from 1.4 to 58 ng/mL, which is slightly higher than the theoretical range of 0.3 to 44 ng/mL. The  $\delta$ -values were not available for these water samples.

The river water samples from Norwegian rivers showed boron concentrations between 3 and 39 ng/mL, with  $\delta^{11}\text{B}$  values ranging from 1 to 11‰. With the theoretical boron concentration of 1.0 to 200 ng/mL falling within this range. In a study by Bolan et al., 2023, rivers in Great Britain show a boron concentration of 15 to 96 ng/mL, and in Rhine and Meuse rivers in Netherlands a concentration of 40 to 200 ng/mL, and in China 2-510 ng/mL (Bolan et al., 2023). This shows that boron concentrations in rivers can vary widely depending on the geographical region of interest. The  $\delta^{11}\text{B}$  values observed were within the wide range of theoretical  $\delta$ -values.

#### **4.7 Method Development**

To have a broad preliminary understanding of the method and its utility in measuring boron concentrations, it was used measuring atomic concentrations of boron on HR-ICP-MS. This was done to know the concentration of the samples prior to analyzing them by isotope analysis on MC-ICP-MS to calculate the recovery rates. Too high concentrations were consequently diluted to the desired concentration and calculated back to its original concentration.

For the study where boron concentrations were held constant but changing the salt concentration with 3% NaCl, it was found that most of the boron was found in the elute solution and nothing to little boron in the wash solution regardless of NaCl solution. After this, boron was varied but the salt concentration was held constant, and the results showed the same, indicating that varying salt concentration or boron concentration in comparison to each other, do not affect the method significantly.

Throughout the analyses by MC-ICP-MS, recovery rates started declining over time, making the  $\delta^{11}\text{B}$ -values and concentration data increasingly uncertain. Evaporation as a function of how much sample remained in the PFA vial was also tested to see if doing this could improve recovery rates (Figure 12).

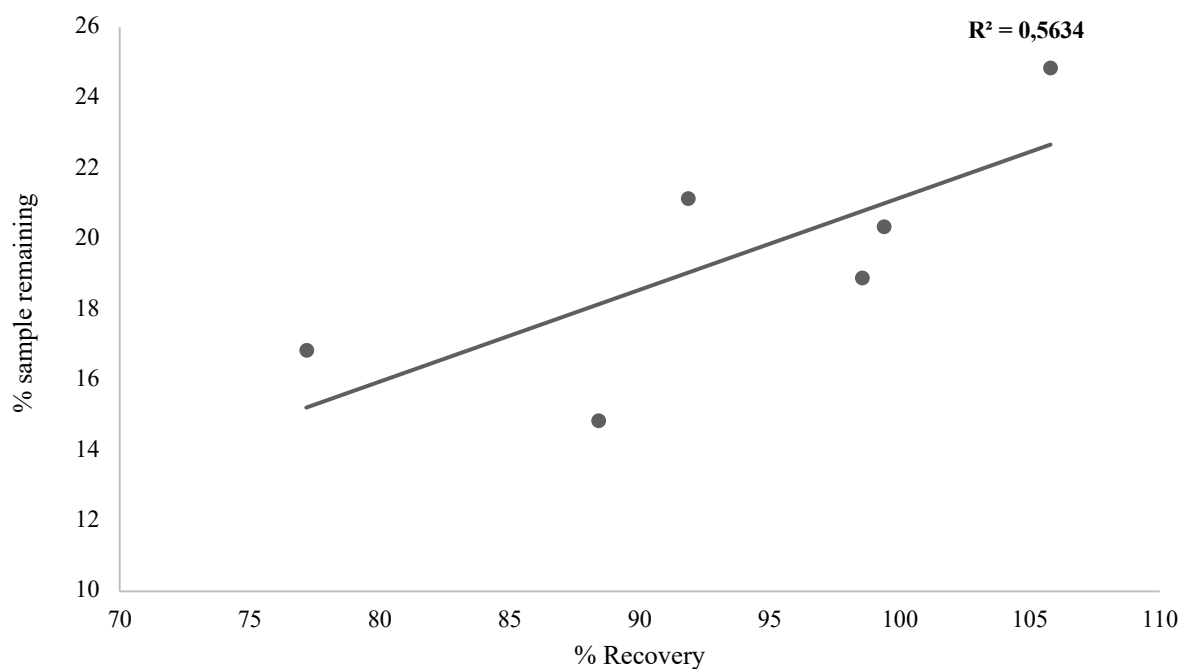


**Figure 12** – Percentage of remaining sample plotted against % recovery. The graph shows a  $R^2 = 0.56$ , indicating a moderate positive correlation between sample remaining and recovery rates.

As seen in Figure 12, there is a moderate positive correlation between recovery rates and sample remaining after evaporation. It seems that at 25% sample remaining, recovery is >100%. However, some of the samples that were not evaporated also showed 100% recovery. Evaporation tests suggested that there was a positive relationship between sample up to 25 % remaining and recovery, however, this step was time-consuming and samples without evaporation also showed high recovery rates in some cases.

When measuring low concentrations of boron together with 2.5 ng/mL boron from  $\text{HNO}_3$  2 mol/L, this significantly increases the background boron levels. To increase the ratio between background noise and sample intensity, the prepFAST system was programmed to flush the column three times with the sample instead of one. However, the results showed that it did not

improve the method in comparison to one cycle, which was also shown in de la Vega et al., 2020. To lower the time spent on the prepFAST, one cycle was used for the rest of the samples.

## 5. Conclusion

This thesis applied and optimized a method for boron isotope analysis in various aqueous matrices, aligning with the broader goals of the MetroPOEM project. Boron concentrations and  $\delta^{11}\text{B}$  values across the matrices generally aligned with theoretical values, effectively addressing **Research Question 1**. The findings confirmed that the method met **Research Criteria 1**, achieving a limit of detection (LOD) of 1.4 ng/mL. This level of sensitivity makes the method applicable to a wide range of concentrations and aqueous matrices. However, the recovery rates were variable and did not consistently reach 100% for all measurements, thereby not fulfilling **Research Criteria 3**. A plausible explanation for the inconsistent recovery rates is the sample pH of 5.5. Literature suggests that an alkaline solution is more effective for the chromatographic separation of boron using the IRA743 resin. The low recovery rates likely contributed to not meeting **Research Criteria 2**, concerning the precision of the method, as the standard deviation between replicates'  $\delta^{11}\text{B}$  values exceeded 5‰ for some samples. Also the method did not meet **Research Criteria 4** either, achieving  $\delta^{11}\text{B}$  values within a 1‰ standard deviation for the CRM AE123. Again, this might be attributable to the recovery rates for these measurements, which were variable. Overall, the method was applicable to various concentrations of boron in different aqueous matrices with satisfactory sensitivity and accuracy. However, the issues with precision and recovery rates indicate that the method requires further optimization. Therefore, the method cannot yet be regarded as fully successful in its application to aqueous matrices.

## 6. Further Work

Further studies should focus on decreasing reagent background levels to reduce the signal-to-noise ratio for lower concentration samples and to lower the method LOD/LOQ. This would allow analysis of lower concentration samples, e.g. lake water samples, which were analyzed but excluded from this analysis due to being <LOD. A plausible explanation for the high LOD and LOQ is the high concentrations of boron found in the two ammonium acetate reagents used, having concentrations of 11 and 3.9 ng/mL respectively. Further studies should also

consider changing the column as the recovery rates starts to decline. To increase the recovery, it could also be interesting to look at how a sample with pH = 8 (or in the range between 5.5 used in this study and 8) would influence the recovery as boron will be found as the borate anion and binds more readily with the column. Additional analyses of samples from other aqueous matrices as well as more data concerning the matrices analyzed here, would advance knowledge of  $\delta^{11}\text{B}$ -values and concentrations in various geological contexts and lower the large standard deviations shown here. This can potentially be used in tracing pollutants in the industrial water back to the industrial source.

## 7. References

- Arunkumar B, Thippeshappa G, Anjali M, Prashanth K (2018). Boron: A critical micronutrient for crop growth and productivity. *J Pharmacognosy Phytochemistry*, 7, 2738–2741.
- Bai, C., Li, K., Fang, D., Ye, X., Zhang, H., Li, Q., Li, J., Liu, H., & Wu, Z. (2021). Efficient separation of boron from salt lake brine using a novel flotation agent synthesized from NMDG and 1-bromooctadecane. *Colloids and Surfaces A: Physicochemical and Engineering Aspects*, 627, 127178. <https://doi.org/10.1016/j.colsurfa.2021.127178>
- Barth, S. (1998). Application of boron isotopes for tracing sources of anthropogenic contamination in groundwater. *Water Research*, 32(3), 685–690. [https://doi.org/10.1016/S0043-1354\(97\)00251-0](https://doi.org/10.1016/S0043-1354(97)00251-0)
- Bin Darwish, N., Kochkodan, V., & Hilal, N. (2015). Boron removal from water with fractionized Amberlite IRA743 resin. *Desalination*, 370, 1–6. <https://doi.org/10.1016/j.desal.2015.05.009>
- Bolan, S., Wijesekara, H., Amarasiri, D., Zhang, T., Ragályi, P., Brdar-Jokanović, M., Rékási, M., Lin, J. Y., Padhye, L. P., Zhao, H., Wang, L., Rinklebe, J., Wang, H., Siddique, K. H. M., Kirkham, M. B., & Bolan, N. (2023). Boron contamination and its risk management in terrestrial and aquatic environmental settings. *The Science of the Total Environment*, 894, 164744. <https://doi.org/10.1016/j.scitotenv.2023.164744>

Crumpton-Banks, J. G. M., & Rae, J. W. B. (2020). SIDEBAR. Boron isotopes provide insights into biomineralization, seawater pH, and ancient atmospheric CO<sub>2</sub>. *Oceanography*, 33. <https://doi.org/10.5670/oceanog.2020.222>

Darvell, B. W. (2018). More chemistry. In B. W. Darvell (Ed.), *Materials science for dentistry* (10th ed., pp. 771–789). Woodhead Publishing. <https://doi.org/10.1016/B978-0-08-101035-8.50030-4>

de la Vega, E., Foster, G. L., Martínez-Botí, M. A., & et al. (2020). Automation of boron chromatographic purification for  $\delta^{11}\text{B}$  analysis of coral aragonite. *Rapid Communications in Mass Spectrometry*, 34(e8762). <https://doi.org/10.1002/rcm.8762>

Dotsika, E., Poutoukis, D., Michelot, J. L., & others. (2006). Stable isotope and chloride, boron study for tracing sources of boron contamination in groundwater: Boron contents in fresh and thermal water in different areas in Greece. *Water, Air, & Soil Pollution*, 174(1–4), 19–32. <https://doi.org/10.1007/s11270-005-9015-8>

Duxbury, A. C., Byrne, R. H., & Mackenzie, F. T. (2024, July 11). Seawater. Encyclopedia Britannica. <https://www.britannica.com/science/seawater>

Farhat, A., Ahmad, F., & Arafat, H. (2013). Analytical techniques for boron quantification supporting desalination processes: A review. *Desalination*, 310, 9–17. <https://doi.org/10.1016/j.desal.2011.12.020>

Foster, G.L., Lécuyer, C., Marschall, H.R. (2018). Boron Stable Isotopes. In: White, W.M. (eds) *Encyclopedia of Geochemistry*. Encyclopedia of Earth Sciences Series. Springer, Cham. [https://doi.org/10.1007/978-3-319-39312-4\\_238](https://doi.org/10.1007/978-3-319-39312-4_238)

Foster, G. L., von Strandmann, P. A. E., & Rae, J. W. B. (2010). Boron and magnesium isotopic composition of seawater. *Geochemistry, Geophysics, Geosystems*, 11(8), Q08015. <https://doi.org/10.1029/2010GC003201>

Foster, G.L., Lécuyer, C., Marschall, H.R. (2016). Boron Stable Isotopes. In: White, W. (eds) *Encyclopedia of Geochemistry*. Encyclopedia of Earth Sciences Series. Springer, Cham. [https://doi.org/10.1007/978-3-319-39193-9\\_238-1](https://doi.org/10.1007/978-3-319-39193-9_238-1)

- He, M. Y., Li, D., Lu, H., & Jin, Z. D. (2019). Elimination of the boron memory effect for rapid and accurate boron isotope analysis by MC-ICP-MS using NaF. *Journal of Analytical Atomic Spectrometry*, 34, 1026–1032. <https://doi.org/10.1039/C9JA00007K>
- Hoefs, J. (2015). *Stable isotope geochemistry* (7th ed.). Springer, Cham.
- Hudec, M. R. (2023). What are mud volcanoes? The Conversation. <https://theconversation.com/what-are-mud-volcanoes-173198>
- Jensen, K. A. (2023). Induktivt koblet plasma massespektrometri. In KJM340 Instrumentell uorganisk analyse. Norwegian University of Life Sciences, Ås, Norway.
- Jerome, S. (2023). Uncertainties and statistics. In KJM350 Radiokjemi. Norwegian University of Life Sciences, Ås, Norway.
- Kopf, A., & Deyhle, A. (2002). Back to the roots: Boron geochemistry of mud volcanoes and its implications for mobilization depth and global B cycling. *Chemical Geology*, 192(3–4), 195–210. [https://doi.org/10.1016/S0009-2541\(02\)00221-8](https://doi.org/10.1016/S0009-2541(02)00221-8)
- Kowalski, P. M., Wunder, B., & Jahn, S. (2013). Ab initio prediction of equilibrium boron isotope fractionation between minerals and aqueous fluids at high P and T. *Geochimica et Cosmochimica Acta*, 101, 285–301. <https://doi.org/10.1016/j.gca.2012.10.007>
- Landsman, M. R., Rivers, F., Pedretti, B. J., Freeman, B. D., Lawler, D. F., Lynd, N. A., & Katz, L. E. (2021). Boric acid removal with polyol-functionalized polyether membranes. *Journal of Membrane Science*, 638, 119690. <https://doi.org/10.1016/j.memsci.2021.119690>
- Mao, H.-R., Liu, C.-Q., & Zhao, Z.-Q. (2019). Source and evolution of dissolved boron in rivers: Insights from boron isotope signatures of end-members and model of boron isotopes during weathering processes. *Earth-Science Reviews*, 190, 439–459. <https://doi.org/10.1016/j.earscirev.2019.01.016>
- Marschall, H. R., & Foster, G. L. (2018). *Boron isotopes: The fifth element*. Springer. <https://doi.org/10.1007/978-3-319-64666-4>
- Marshall, A. G., Blakney, G. T., Chen, T., Kaiser, N. K., McKenna, A. M., Rodgers, R. P., Ruddy, B. M., & Xian, F. (2013). Mass resolution and mass accuracy: How much is enough?

*Mass Spectrometry (Tokyo, Japan)*, 2(Spec Iss), S0009.

<https://doi.org/10.5702/massspectrometry.S0009>

Millot, R., Hegan, A., & Négrel, P. (2012). Geothermal waters from the Taupo Volcanic Zone, New Zealand: Li, B and Sr isotopes characterization. *Applied Geochemistry*, 27(3), 677–688. <https://doi.org/10.1016/j.apgeochem.2011.12.015>

Neufeld, L. (2019). ICP-MS interface cones: Maintaining the critical interface between the mass spectrometer and the plasma discharge to optimize performance and maximize instrument productivity. *Spectroscopy*, 34(7), 12–17. Retrieved from <https://www.spectroscopyonline.com/view/icp-ms-interface-cones-maintaining-critical-interface-between-mass-spectrometer-and-plasma-discharge>

Rivas, S., Sanchez-Alfaro, P., Alvarez-Amado, F., Perez-Fodich, A., Godfrey, L., Becerra, P., Tardani, D., Perez-Flores, P., Aron, F., Fica, C., Munoz-Saez, C., & Mathur, R. (2024). Water-rock interaction and magmatic contribution in thermal fluids of the Southern Volcanic Zone, Chile: Insights from Li, B and Sr isotopes. *Journal of Volcanology and Geothermal Research*, 453, 108149. <https://doi.org/10.1016/j.jvolgeores.2024.108149>

Saldi, G. D., Noireaux, J., Louvat, P., Faure, L., Balan, E., Schott, J., & Gaillardet, J. (2018). Boron isotopic fractionation during adsorption by calcite – Implication for the seawater pH proxy. *Geochimica et Cosmochimica Acta*, 240, 255–273. <https://doi.org/10.1016/j.gca.2018.08.025>

Sankoh, A. A., Derkyi, N. S. A., Frazer-Williams, R. A. D., Laar, C., & Kamara, I. (2022). A review on the application of isotopic techniques to trace groundwater pollution sources within developing countries. *Water*, 14(1), 35. <https://doi.org/10.3390/w14010035>

Schlesinger, W. H., and A. Vengosh (2016), Global boron cycle in the Anthropocene, *Global Biogeochem. Cycles*, 30, 219–230, doi:[10.1002/2015GB005266](https://doi.org/10.1002/2015GB005266).

Schönbächler, M. (2018). Inductively coupled plasma mass spectrometry (ICP-MS). In W. M. White (Ed.), *Encyclopedia of Geochemistry (Encyclopedia of Earth Sciences Series)*. Springer, Cham. [https://doi.org/10.1007/978-3-319-39312-4\\_111](https://doi.org/10.1007/978-3-319-39312-4_111)

Tiwari, M., Singh, A. K., & Sinha, D. K. (2015). Stable isotopes: Tools for understanding past climatic conditions and their applications in chemostratigraphy. In M. Ramkumar (Ed.), *Chemostratigraphy* (pp. 65–92). Elsevier. <https://doi.org/10.1016/B978-0-12-419968-2.00003-0>

Wilschefski, S. C., & Baxter, M. R. (2019). Inductively coupled plasma mass spectrometry: Introduction to analytical aspects. *The Clinical Biochemist Reviews*, 40(3), 115–133. <https://doi.org/10.33176/AACB-19-00024>

Wei, H.-Z., Jiang, S.-Y., Yang, T.-L., Yang, J.-H., Yang, T., Yan, X., Ling, B.-P., Liu, Q., & Wu, H.-P. (2014). Effect of metasilicate matrices on boron purification by Amberlite IRA 743 boron specific resin and isotope analysis by MC-ICP-MS. *Journal of Analytical Atomic Spectrometry*, 29(11). <https://doi.org/10.1039/C4JA00153B>

## Appendix A - Data Manipulation and Calculations

### 1. Instrument blank correction and calculating uncorrected $\delta^{11}\text{B}$

The 100 ng/mL NIST951a with 17.5 ng/mL boron 1 and 2 as well as MQ-H<sub>2</sub>O 1 is corrected for by the instrument blank which consists of 2% HNO<sub>3</sub>. This is done by subtracting the instrument blank's value from the <sup>10</sup>B and <sup>11</sup>B intensity, and done for all samples and NIST<sub>951a</sub> standards (see Figure VX).

	A	B	C	D	E	F	G	H	I	J	K	L
1								Instrument blank correction				
2			10B	11B	10B/11B	11B/10B		10B	11B	11B/10B		$\delta^{11}\text{B}$
3		Blank 1										
4		Mean	0,003	0,016		4,863						
5		Std (abs)	0,000	0,000		0,009						
6												
7		100 ppb NIST951a 1										
8		Mean	0,063	0,314		5,027		0,06	0,30	5,04		
9		Std (abs)	0,001	0,003		0,000						
10												
11		Blank 2										
12		Mean	0,003	0,012		4,841						
13		Std (abs)	0,000	0,000		0,010						
14		rsd (%)										
15	1,00	MQ-H <sub>2</sub> O 1										
16		Mean	0,005	0,025		4,946		0,00	0,01	5,05		2,33
17		Std (abs)	0,000	0,000		0,004						
18		rsd (%)										
19		Blank 3										
20		Mean	0,002	0,008		4,785						
21		Std (abs)	0,000	0,000		0,017						
22												
23		100 ppb NIST951a 2										
24		Mean	0,063	0,316		5,033		0,06	0,31	5,04		
25		Std (abs)	0,001	0,004		0,001						
26												

**Figure V1** – A screenshot from Microsoft Excel showing how the samples were subtracted by the instrument blank, and a  $\delta^{11}\text{B}$ -value was calculated.

The  $\delta^{11}\text{B}$ -value is calculated by taking the corrected sample's <sup>11</sup>B/<sup>10</sup>B ratio and dividing it by the mean of the <sup>11</sup>B/<sup>10</sup>B ratio for each of the two NIST<sub>951a</sub> standards. Keep in mind that these two standards have also been corrected for by the instrument blank. Then this value is subtracted by 1, and multiplied by 1000 to get it into permille (‰).

### 2. Calculating concentration (ng/mL) from intensity

A table is made of all the NIST<sub>951a</sub> standards' <sup>11</sup>B intensities in the analysis. These are all already corrected for the instrument blank like in step 1. The mean of all the instrument blank corrected <sup>11</sup>B intensities of the standards in the analyses is calculated. This is the average intensity of the <sup>11</sup>B signal from the 100 ng/mL NIST<sub>951a</sub> standard containing 17.5 ng/mL

boron. The mean is then divided by 17.5 which gives the average intensity of  $^{11}\text{B}$  1.0 ng/mL boron in the standard.

<b>NIST951a</b>	
<b>n</b>	<b>Intensity instrumental blank correction</b>
1,00	0,30
2,00	0,31
3,00	0,30
4,00	0,31
5,00	0,31
6,00	0,31
7,00	0,31
8,00	0,30
9,00	0,30
10,00	0,21
11,00	0,20
12,00	0,20
13,00	0,19
14,00	0,20
15,00	0,19
16,00	0,19
17,00	0,18
18,00	0,17
19,00	0,17
20,00	0,21
21,00	0,21
22,00	0,21
23,00	0,20
24,00	0,20
25,00	0,21
<b>Average Intensity 17.5 ppb</b>	<b>0,24</b>
<b>Average Intensity 1 ppb</b>	<b>0,01</b>

**Figure V2** – A screenshot from Microsoft Excel showing how the standards'  $^{11}\text{B}$  intensities were collected into a table, to find the average intensity of 17.5 ng/mL boron and 1.0 ng/mL boron.

Then all the intensities of the samples are written in a new table. However, these signal intensities have only been corrected for the instrument blank, and they also need to be corrected for the sample's blank intensities by subtraction. The sample blanks are Milli-Q with ammonium acetate and nitric acid, that have also gone through the ion exchange chromatography on the prepFAST. By subtracting the Milli-Q sample blanks corrected by the instrument blank and subtract it by the intensities of the Milli-Q samples also corrected for the instrument blank, this gives the true  $^{11}\text{B}$  signal intensity of the actual sample (see Figure V3).

ID	intensity instrumental blank correction	intensity sample blank correction	ppb corrected	Dilution	ppb expected	ppb measured	Recovery
2023-136-001	0.20	0.18	13.76	10.00	222.8125	137.59	62
2023-138-004	0.39	0.37	27.38	1	413	27.38	7
2023-135-020	0.27	0.24	17.85	10	225	178.46	79
2023-135-007	0.06	0.03	2.26	10.00	75	22.56	30
2023-074-002	0.24	0.22	16.53	10.00	234	165.30	71
2023-126-011	0.36	0.34	25.17	1.00	200	25.17	13
2023-126-012	0.15	0.13	9.76	1.00	200	9.76	5
2023-061-012	0.15	0.13	9.84	1.00	200	9.84	5
AE120	0.26	0.25	18.27	10	206.25	182.75	89
AE121	0.26	0.25	18.29	10	210	182.90	87
AE122	0.29	0.27	20.01	25	675	500.23	74
AE123	0.19	0.18	13.02	10.00	187.5	130.23	69

**Figure V3** – A screenshot from Microsoft Excel showing how the standards'  $^{11}\text{B}$  intensities were collected into a table, to find the average intensity of 17.5 ng/mL boron and 1.0 ng/mL boron.

Then these  $^{11}\text{B}$  signal intensities are converted into ng/mL by dividing the intensities by the number calculated as the average intensity of 1.0 ng/mL boron in the standard. If the sample has been diluted during the analysis, due to the signal being saturated, it is multiplied with the dilution factor to get the original concentration of the sample.

### 3. Calculating recovery

To find the recovery the measured concentration value in ng/mL is divided by the theoretical diluted concentration in the prepFAST sample and multiplied by 100%.

To correct the recovery with a sample, a CRM with a known concentration could be used, but was not done here. The measured concentration in ng/mL of the reference material is divided by the theoretical expected concentration times 100. Then 100 is divided by this number, and multiplied with each recovery value to get the corrected recovery value.

### 4. $\delta^{11}\text{B}$ -blank correction

1. The  $^{11}\text{B}$  intensity of each blank is written down in a list (A).
2. In a new column the  $\delta^{11}\text{B}$ -values of the blanks are written down (X).
3. Each blank's  $^{11}\text{B}$  intensity is subtracted from sample's  $^{11}\text{B}$  intensity, and multiplied by the dilution (B).
4. Then column A and B is added in a new column (A+B).
5. In a final column the  $\delta^{11}\text{B}$ -values of the samples are written down (Z).
6. → The  $\delta^{11}\text{B}$ -blank-correction is found by taking:

$$\frac{((A + B)Z) - (A - X)}{B}$$

7. To find the signal-to-noise ratio. The value from point 3 (B) is divided by point 1 (A). → B/A

This means the  $^{11}\text{B}$  intensity value of the sample having the blank subtracted from it divided by the intensity of  $^{11}\text{B}$  for the blank. Figure V4 shows how this would look like in a table.

Delta correction									
ID	Dilution	A	X	B	A+B	Z	Y	Signal/noise	
2023-136-001	10	0,02	-0,13	1,85	1,87	37,85	38,21	107,24	
2023-138-004	1	0,02	2,78	0,37	0,39	7,61	7,83	21,66	
2023-135-020	10	0,03	17,04	2,40	2,43	4,12	3,96	80,40	
2023-074-002	10	0,02	3,98	2,22	2,24	6,15	6,17	109,22	
2023-126-011	1	0,02	3,57	0,34	0,36	4,22	4,26	15,86	
2023-126-012	1	0,02	4,03	0,31	0,33	5,84	5,96	14,73	
2023-61-012	25	0,02	5,09	3,31	3,33	5,88	5,88	168,35	
2023-135-007	10	0,03	9,57	0,30	0,33	11,71	11,89	11,62	
AE120	10	0,01	2,33	2,46	2,47	-24,02	-24,16	188,36	
AE121	10	0,02	-6,05	2,46	2,48	16,20	16,36	136,18	
AE122	25	0,02	2,77	6,70	6,72	36,59	36,68	377,50	
AE123	10	0,02	6,57	1,75	1,77	-1,35	-1,42	107,49	

**Figure V4** – A screenshot from Microsoft Excel showing the  $\delta^{11}\text{B}$ -values corrected for the blank and a signal-to-noise ratio can be calculated.

### 5. $\delta^{11}\text{B}$ reference material correction

The  $\delta^{11}\text{B}$  -values in which are corrected for blanks are written down in a column. In another column, the true known values of the reference materials AE120, AE121 and AE122 is written down. Then the slope and intercept are found by using excel of these three points. The correction is done by taking the  $\delta^{11}\text{B}$ -value and multiplying it with the slope of the line, and adding the intercept-value.

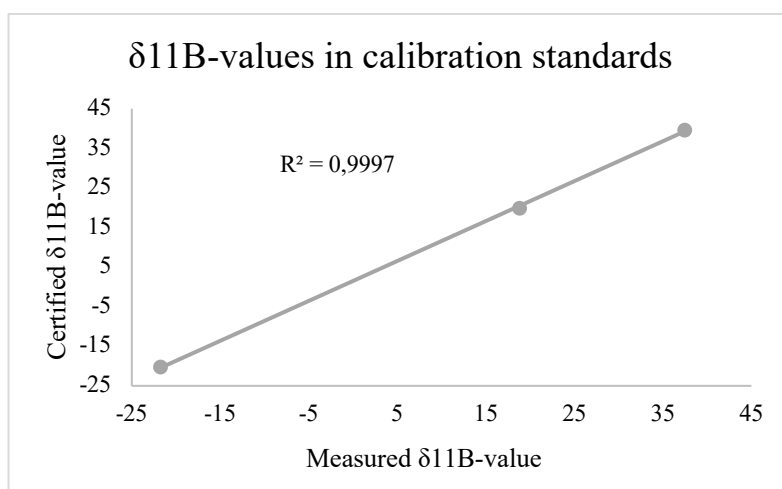


**Figure V5** – An example of a graph showing the relationship between the certified  $\delta^{11}\text{B}$ -value and measured  $\delta^{11}\text{B}$ -value. In this analysis the  $R^2$  is 1.0, which indicates a strong relationship.

The slope and intercept of this line is used to correct the  $\delta^{11}\text{B}$ -values using the certified  $\delta^{11}\text{B}$ -values of the CRMs, AE120-122.

## **6. Dilutions**

All volume/volume (v/v) and weight/volume (w/v) dilutions were made using the formula  $C_1V_1 = C_2V_2$ . Dilutions were made using Milli-Q water.

## **7. LOD and LOQ calculations**

The three last analyses all used all CRMs and alternating blanks and are representative of the final method. Because of this the alternating blanks in each respective analysis were put into a table, and a LOD and LOQ was calculated individually for the analyses.

The LOD is defined as three times the standard deviation of the blanks, and the LOQ as ten times the standard deviation of the blanks. Because of this the mean for each of the analyses' blanks were calculated, followed by calculating the standard deviation and multiplying this by 3 and 10. To calculate a common method LOD and LOQ, the mean of the LOD and LOQ was found and used as the final LOD and LOQ.

In these three analyses some samples were diluted because of the signal intensity being saturated (above 0.5 V). In this case the LOD would be multiplied by the dilution factor and become higher. In some cases, this would result in the LOD being higher than the sample's concentration, even though the sample's original concentration is in fact over the LOD. To avoid this, all the diluted concentrations were multiplied back to their original concentration.

## Appendix B – Raw Data

**Table V1** – Raw data showing personally analyzed samples. The table includes number of samples, ID of the sample, sample type., measured concentration in (ng/mL), recovery rates, signal-to-noise ratio,  $\delta^{11}\text{B}$ -value, reference materials used in the analyses and blanks used.

Number of samples	ID	Date analyzed	Sample type	Sample comment	Measured concentration (ng/mL)	Recovery (%)	Signal/noise	$\delta^{11}\text{B}$	Reference material used for delta correction	Blank used	Reference materials used
1	AE121	26/04/2024	Reference material		527,95	251	138,22	18,66	No correction due to too low concentration	Alternating	AE120, AE121, AE122, AE123
2	AE120	26/04/2024	Reference material		503,13	244	179,60	-21,59	No correction due to too low concentration	Alternating	AE120, AE121, AE122, AE123
3	AE122	17/04/2024	Reference material		500	74	377,50	39,79	AE120, AE121, AE122	Alternating	AE120, AE121, AE122, AE123
4	AE121	20/03/2024	Reference material		325	155	116,36	14,25	AE120, AE121, AE122	4 blanks	AE120, AE121, AE122
5	AE120	20/03/2024	Reference material		293	142	104,94	-17,53	AE120, AE121, AE122	4 blanks	AE120, AE121, AE122
6	AE121	17/04/2024	Reference material		183	87	136,18	19,77	AE120, AE121, AE122	Alternating	AE120, AE121, AE122, AE123
7	AE120	17/04/2024	Reference material		183	89	188,36	-20,16	AE120, AE121, AE122	Alternating	AE120, AE121, AE122, AE123
8	2023-135-020	17/04/2024	Landfill Leachate	GLT/Horison Landfill	178	79	80,40	7,55	AE120, AE121, AE122	Alternating	AE120, AE121, AE122, A123
9	AE122	26/04/2024	Reference material		170,38	25	47,05	36,77	No correction due to too low concentration	Alternating	AE120, AE121, AE122, AE123
10	2023-126-011	17/04/2024	Landfill Leachate	IRMAT Landfill	165	71	15,86	7,84	AE120, AE121, AE122	Alternating	AE120, AE121, AE122, A123
11	2023-136-001	17/04/2024	Seawater	North Sea	138	62	107,24	41,29	AE120, AE121, AE122	Alternating	AE120, AE121, AE122, A123
12	2023-144-004	20/03/2024	Landfill Leachate	IRMAT Landfill	134	60	48,03	6,57	AE120, AE121, AE122	4 blanks	AE120, AE121, AE122
13	AE123	17/04/2024	Reference material		130	69	107,49	2,25	AE120, AE121, AE122	Alternating	AE120, AE121, AE122, AE123
14	AE122	05/04/2024	Reference material		119	176	-174,82	37,19	AE120, AE121, AE122	Alternating	AE120, AE121, AE122, AE123
15	2023-138-003	20/03/2024	Landfill Leachate	Esva Landfill	105	46	37,42	6,73	AE120, AE121, AE122	4 blanks	AE120, AE121, AE122
16	2023-126-012	12/03/2024	Landfill Leachate	Øras Landfill	87,96	59	14,24	-1,61	No correction due to too high blank	1 Blank	AE123
17	2023-138-004	12/03/2024	Landfill Leachate	Esva Landfill	81,76	55	13,24	4,34	No correction due to too high blank	1 Blank	AE123
18	2023-109-042	10/01/2024	Seawater	Mediterranean sea, Greece	66	344		35,38	AE120, AE121, AE122	No blank	AE120, AE121, AE122
19	2023-126-011	05/04/2024	Landfill Leachate	Øras Landfill	65	33	30,79	5,86	AE120, AE121, AE122	Alternating	AE120, AE121, AE122, AE123
20	2023-126-012	05/04/2024	Landfill Leachate	Øras Landfill	65	32	3,19	4,59	AE120, AE121, AE122	Alternating	AE120, AE121, AE122, AE123
21	2023-138-004	05/04/2024	Landfill Leachate	Esva Landfill	62	15	31,68	9,76	AE120, AE121, AE122	Alternating	AE120, AE121, AE122, AE123
22	2023-060-009	20/03/2024	Landfill Leachate	Sirkula IKS	58	26	20,70	10,95	AE120, AE121, AE122	4 blanks	AE120, AE121, AE122
23	2023-061-012	05/04/2024	Landfill Leachate	Øras	49	25	2,20	4,69	AE120, AE121, AE122	Alternating	AE120, AE121, AE122, AE123
24	2023-109-027	10/01/2024	Groundwater	Well - Greece	44	117		12,63	AE120, AE121, AE122	No blank	AE120, AE121, AE122
25	2023-109-010	10/01/2024	Groundwater	Well - Greece	43	115		21,49	AE120, AE121, AE122	No blank	AE120, AE121, AE122
26	2023-109-016	10/01/2024	Groundwater	Well - Greece	40	108		12,63	AE120, AE121, AE122	No blank	AE120, AE121, AE122
27	AE121	05/04/2024	Reference material		40	19	33,80	23,34	AE120, AE121, AE122	Alternating	AE120, AE121, AE122, AE123

28	2023-109-032	10/01/2024	Groundwater	Well - Greece	38	119		20,65	AE120, AE121, AE122	No blank	AE120, AE121, AE122
29	2023-109-005	10/01/2024	Groundwater	Well - Greece	38	101		11,49	AE120, AE121, AE122	No blank	AE120, AE121, AE122
30	2023-109-038	10/01/2024	Groundwater	Borehole - Greece	38	126		35,85	AE120, AE121, AE122	No blank	AE120, AE121, AE122
31	2023-136-001	20/03/2024	Seawater	North Sea	38	17	13,43	43,10	AE120, AE121, AE122	4 blanks	AE120, AE121, AE122
32	2023-109-012	10/01/2024	Groundwater	Well - Greece	37	98		22,43	AE120, AE121, AE122	No blank	AE120, AE121, AE122
33	2023-109-034	10/01/2024	Groundwater	Borehole - Greece	37	88		45,02	AE120, AE121, AE122	No blank	AE120, AE121, AE122
34	2023-109-037	10/01/2024	Groundwater	Borehole - Greece	36	118		21,55	AE120, AE121, AE122	No blank	AE120, AE121, AE122
35	2023-109-040	10/01/2024	Groundwater	Borehole - Greece	35	92		37,57	AE120, AE121, AE122	No blank	AE120, AE121, AE122
36	2023-109-007	10/01/2024	Groundwater	Well - Greece	34	91		24,75	AE120, AE121, AE122	No blank	AE120, AE121, AE122
37	2023-109-003	10/01/2024	Groundwater	Well - Greece	33	89		10,00	AE120, AE121, AE122	No blank	AE120, AE121, AE122
38	2023-109-042	20/03/2024	Seawater	Mediterranean - Greece	33	15	11,68	44,91	AE120, AE121, AE122	4 blanks	AE120, AE121, AE122
39	2023-109-023	10/01/2024	Groundwater	Well - Greece	32	84		16,86	AE120, AE121, AE122	No blank	AE120, AE121, AE122
40	2023-116-001	20/03/2024	Landfill Leachate	Esval Landfill	31	14	11,05	16,72	AE120, AE121, AE122	4 blanks	AE120, AE121, AE122
41	2023-136-001	05/04/2024	Seawater	North Sea	28	13	1,62	66,34	AE120, AE121, AE122	Alter nating	AE120, AE121, AE122, AE123
42	2023-138-004	17/04/2024	Landfill Leachate	Esval Landfill	27	7	21,66	11,37	AE120, AE121, AE122	Alter nating	AE120, AE121, AE122, A123
43	2023-109-018	10/01/2024	Groundwater	Well - Greece	27	72		11,98	AE120, AE121, AE122	No blank	AE120, AE121, AE122
44	2023-109-039	10/01/2024	Groundwater	Borehole - Greece	26	70		35,53	AE120, AE121, AE122	No blank	AE120, AE121, AE122
45	2023-136-001	10/01/2024	Seawater	North Sea	26	78		38,84	AE120, AE121, AE122	No blank	AE120, AE121, AE122
46	2023-074-002	05/04/2024	Landfill Leachate	IRMAT Landfill	26	11	1,34	6,16	AE120, AE121, AE122	Alter nating	AE120, AE121, AE122, AE123
47	2023-109-042	10/01/2024	Seawater	Mediterranean sea, Greece	25	67		32,53	AE120, AE121, AE122	No blank	AE120, AE121, AE122
48	2023-126-012	17/04/2024	Landfill Leachate	Øras Landfill	25	13	14,73	9,52	AE120, AE121, AE122	Alter nating	AE120, AE121, AE122, A123
49	AE120	05/04/2024	Reference material		25	12	14,50	- 22,93	AE120, AE121, AE122	Alter nating	AE120, AE121, AE122, AE123
50	AE123	05/04/2024	Reference material		25	13	1,52	- 12,49	AE120, AE121, AE122	Alter nating	AE120, AE121, AE122, AE123
51	2023-074-002	17/04/2024	Landfill Leachate	IRMAT Landfill	23	30	109,22	9,72	AE120, AE121, AE122	Alter nating	AE120, AE121, AE122, A123
52	AE122	20/03/2024	Reference material		22	11	7,95	42,68	AE120, AE121, AE122	4 blanks	AE120, AE121, AE122
53	2023-135-020	05/04/2024	Landfill Leachate	GLT/Horisont Landfill	21	9	6,02	0,66	AE120, AE121, AE122	Alter nating	AE120, AE121, AE122, AE123
54	AE123	12/03/2024	Reference material		14,99	60	2,43	- 0,74	No correction due to too high blank	1 Blank	AE123
55	2023-109-042	12/03/2024	Seawater	Mediterranean, Greece	13,96	10	2,26	31,08	No correction due to too high blank	1 Blank	AE123
56	AE122	01/03/2024	Reference material		13,90	69	4,52	40,83	No correction due to too high blank	1 blank	AE122, NIST951a
57	NIST951a	01/03/2024	Reference material		13,70	91	4,45	- 5,98	No correction due to too high blank	1 blank	AE122, NIST951a
58	2023-060-008	26/04/2024	Groundwater - Monitoring well	Sirkula IKS	11,32	101	3,27	6,47	No correction due to too low concentration	Alter nating	AE120, AE121, AE122, AE123
59	2023-135-007	17/04/2024	Landfill Leachate	Øras	10	5	11,62	15,37	AE120, AE121, AE122	Alter nating	AE120, AE121, AE122, A123
60	2023-61-012	17/04/2024	Landfill Leachate	Øras Landfill	10	5	168,35	9,44	AE120, AE121, AE122	Alter nating	AE120, AE121, AE122, A123

61	2023-077-005	26/04/2024	Urban Water	Nitelva Upstream	7,26	121	1,33	11,23	No correction due to too low concentration	Alter nating	AE120, AE121, AE122, AE123
62	2023-126-005	26/04/2024	Groundwater - Monitoring well	Øras Landfill	6,96	62	2,20	20,99	No correction due to too low concentration	Alter nating	AE120, AE121, AE122, AE123
63	2023-126-004	26/04/2024	Groundwater - Monitoring well	Øras Landfill	5,96	53	1,65	16,46	No correction due to too low concentration	Alter nating	AE120, AE121, AE122, AE123
64	2023-077-003	01/03/2024	Urban Water - River	Leira Downstream	4,79	37	1,56	1,49	No correction due to too high blank	1 blank	AE122, NIST951a
65	NIST951a	01/03/2024	Reference material		4,68	94	1,52	-3,16	No correction due to too high blank	1 blank	AE122, NIST951a
66	2020-129-016	26/04/2024	Groundwater - Monitoring well		4,42	91	1,24	4,52	No correction due to too low concentration	Alter nating	AE120, AE121, AE122, AE123
67	2023-077-002	26/04/2024	Urban Water - River	Glomma river Fetsund	2,36	22	0,96	3,05	No correction due to too low concentration	Alter nating	AE120, AE121, AE122, AE123
68	2023-109-030	10/01/2024	Groundwater	Well - Greece	2,3	6		8,48	AE120, AE121, AE122	No blank	AE120, AE121, AE122
69	NIST951a	01/03/2024	Reference material		1,82	91	0,59	-0,75	No correction due to too high blank	1 blank	AE122, NIST951a
70	AE123	26/04/2024	Reference material		1,22	1	0,03	-2,20	No correction due to too low concentration	Alter nating	AE120, AE121, AE122, AE123
71	2023-135-011	26/04/2024	Groundwater - Monitoring well	GLT/Horisont Landfill	1,02	20	0,24	5,82	No correction due to too low concentration	Alter nating	AE120, AE121, AE122, AE123
72	2023-077-005	01/03/2024	Urban Water	Nitelva Upstream	0,86	5	0,28	-7,16	No correction due to too high blank	1 blank	AE122, NIST951a
73	2023-135-011	01/03/2024	Groundwater - Monitoring well	GLT/Horisont Landfill	0,61	5	0,20	4,89	No correction due to too high blank	1 blank	AE122, NIST951a
74	2023-126-005	01/03/2024	Groundwater - Monitoring well	Øras Landfill	0,51	2	0,16	11,13	No correction due to too high blank	1 blank	AE122, NIST951a
75	2023-126-004	01/03/2024	Groundwater - Monitoring well	Øras Landfill	0,45	2	0,15	9,22	No correction due to too high blank	1 blank	AE122, NIST951a
76	2020-129-016	01/03/2024	Groundwater - Monitoring well		0,44	3	0,14	4,53	No correction due to too high blank	1 blank	AE122, NIST951a
77	2023-077-002	01/03/2024	Urban Water - River	Glomma river Fetsund	0,41	1	0,13	5,61	No correction due to too high blank	1 blank	AE122, NIST951a
78	2023-128-001	12/03/2024	Landfill Leachate	Vestnes Renovasjon Landfill	-0,09	0	-0,01	9,39	No correction due to too high blank	1 Blank	AE123
79	2023-109-009	12/03/2024	Shallow Groundwater	Well - Greece	-2,25	-4	-0,36	5,76	No correction due to too high blank	1 Blank	AE123
80	2023-060-008	01/03/2024	Groundwater - Monitoring well	Sirkula IKS	-2,80	-9	-0,91	66,24	No correction due to too high blank	1 blank	AE122, NIST951a
81	2023-109-002	12/03/2024	Shallow Groundwater	Well - Greece	-4,40	-5	-0,71	3,33	No correction due to too high blank	1 Blank	AE123
82	2023-135-007	05/04/2024	Landfill Leachate	GLT/Horisont Landfill	-6,7	-9	-0,39	9,39	AE120, AE121, AE122	Alter nating	AE120, AE121, AE122, AE123
83	2023-126-011	12/03/2024	Landfill Leachate	Øras Landfill	-12,24	-8	-1,98	0,29	No correction due to too high blank	1 Blank	AE123
84	2023-109-030	12/03/2024	Shallow Groundwater	Well - Greece	-19,68	-33	-3,19	6,81	No correction due to too high blank	1 Blank	AE123

**Table V2** – Overview over the given data, including number of samples , ID, sample type, concentration in the sample (ng/mL) and  $\delta^{11}\text{B}$ -values for the given data.

Number of Samples	Sample ID	Sample Type	Sample Description	Boron Concentration (ng/mL)	$\delta^{11}\text{B}$ (‰)
1	2023-130-003	Mud Volcano	Lusi, Indonesia	102000	
2	2024-002-007	Volcanic Water	Italy	79468,44	23,86
3	2024-002-006	Volcanic Water	Italy	72961,90	24,46
4	2024-002-002	Volcanic Water	Italy	72668,80	34,59
5	2024-002-003	Volcanic Water	Italy	54135,65	22,84
6	2024-002-004	Volcanic Water	Italy	33016,39	42,75
7	2024-002-005	Volcanic Water	Italy	27848,49	42,47
8	2024-002-001	Volcanic Water	Italy	9736,96	53,67
9	2023-109-042	Seawater	Mediterranean, Greece	6413,15	32,67
10	2023-136-001	Seawater	North Sea	5750,00	39,05
11	2023-135-005	Landfill Leachate	GLT/Horizont Landfill	4125,45	1,70
12	2023-135-010	Landfill Leachate	GLT/Horizont Landfill	4042,21	2,64
13	2023-126-011	Landfill Leachate	Øras Landfill	4000,00	0,29
14	2023-126-012	Landfill Leachate	Øras Landfill	4000,00	-1,61
15	2023-138-003	Landfill Leachate	Esval Landfill	4000,00	
16	2023-138-004	Landfill Leachate	Esval Landfill	4000,00	4,34
17	2023-135-015	Landfill Leachate	GLT/Horizont Landfill	3929,08	1,08
18	2023-135-020	Landfill Leachate	GLT/Horizont Landfill	3041,35	1,43
19	2023-109-001	Shallow Groundwater	Well - Greece	844,08	14,24
20	2023-109-023	Shallow Groundwater	Well - Greece	757,42	16,82
21	2023-109-021	Shallow Groundwater	Well - Greece	521,89	
22	2023-109-002	Shallow Groundwater	Well - Greece	503,55	
23	2023-109-003	Shallow Groundwater	Well - Greece	429,35	9,89
24	2023-109-012	Shallow Groundwater	Well - Greece	357,57	22,45
25	2023-109-009	Shallow Groundwater	Well - Greece	331,60	5,76
26	2023-109-041	Shallow Groundwater	Well - Greece	304,58	
27	2023-109-040	Shallow Groundwater	Borehole - Greece	297,50	37,76
28	2023-109-007	Shallow Groundwater	Well - Greece	288,78	24,80
29	2023-109-019	Shallow Groundwater	Well - Greece	257,85	
30	2023-109-030	Shallow Groundwater	Well - Greece	241,38	8,35
31	2023-109-015	Shallow Groundwater	Well - Greece	228,11	
32	2023-109-010	Shallow Groundwater	Well - Greece	224,85	21,50
33	2023-135-018	Groundwater - Monitoring well	GLT/Horizont Landfill	216,04	
34	2023-109-032	Shallow Groundwater	Well - Greece	207,29	20,66
35	2023-130-002	Mud Volcano	Lusi, Indonesia	200	
36	2023-109-026	Shallow Groundwater	Well - Greece	194,23	
37	2023-109-006	Shallow Groundwater	Well - Greece	189,04	
38	2023-109-033	Shallow Groundwater	Well - Greece	177,35	
39	2023-109-024	Shallow Groundwater	Well - Greece	148,53	
40	2023-109-008	Shallow Groundwater	Well - Greece	142,52	13,55
41	2023-109-035	Shallow Groundwater	Borehole - Greece	137,25	
42	2023-109-022	Shallow Groundwater	Well - Greece	134,62	
43	2023-109-034	Shallow Groundwater	Borehole - Greece	122,71	45,30
44	2023-104-027	Urban Water - Storm drain Landfill	Brånäsaldalen landfill	121,42	
45	2023-109-025	Shallow Groundwater	Well - Greece	120,74	
46	2023-109-029	Shallow Groundwater	Well - Greece	118,68	
47	2023-109-013	Shallow Groundwater	Well - Greece	114,26	
48	2023-135-012	Groundwater - Monitoring well	GLT/Horizont Landfill	113,27	
49	2023-109-037	Shallow Groundwater	Borehole - Greece	107,54	21,56
50	2023-109-016	Shallow Groundwater	Well - Greece	105,45	12,54
51	2023-077-086	Urban Water - Storm drain Landfill	Brånäsaldalen landfill	99,47	
52	2023-135-007	Groundwater - Monitoring well	GLT/Horizont Landfill	98,29	0,18
53	2023-109-031	Shallow Groundwater	Well - Greece	95,81	
54	2023-135-013	Groundwater - Monitoring well	GLT/Horizont Landfill	89,77	
55	2023-109-005	Shallow Groundwater	Well - Greece	88,95	11,39
56	2023-109-038	Shallow Groundwater	Borehole - Greece	86,65	36,03
57	2023-109-027	Shallow Groundwater	Well - Greece	80,26	12,55
58	2023-109-004	Shallow Groundwater	Well - Greece	79,74	
59	2023-135-002	Groundwater - Monitoring well	GLT/Horizont Landfill	75,06	
60	2023-135-008	Groundwater - Monitoring well	GLT/Horizont Landfill	73,23	-3,55
61	2023-109-039	Shallow Groundwater	Borehole - Greece	68,80	35,70
62	2023-109-017	Shallow Groundwater	Well - Greece	63,88	
63	2023-104-049	Urban Water - Storm drain Landfill	Brånäsaldalen landfill	60,56	
64	2023-104-005	Urban Water - Storm drain Landfill	Brånäsaldalen landfill	59,73	
65	2023-109-028	Shallow Groundwater	Well - Greece	59,65	
66	2023-104-046	Urban Water - Storm drain Landfill	Brånäsaldalen landfill	58,41	
67	2023-077-020	Lake Water	Romeriksåsen - storovungen	58,18	
68	2023-109-018	Shallow Groundwater	Well - Greece	57,33	11,88
69	2023-077-083	Urban water - storm drain Landfill	Brånäsaldalen landfill	56,33	
70	2023-077-081	Urban Water - Storm drain Landfill	Brånäsaldalen landfill	52,52	
71	2023-077-054	Urban Water - Storm drain Landfill	Brånäsaldalen landfill	51,82	
72	2023-109-036	Shallow Groundwater	Borehole - Greece	51,77	
73	2023-077-009	Urban Water	Brånäsaldalen landfill storm drain surface water	50,84	
74	2023-077-008	Urban Water	Brånäsaldalen landfill storm drain surface water	48,38	
75	2023-104-047	Urban Water - Storm drain Landfill	Brånäsaldalen landfill	48,14	
76	2023-104-004	Urban Water - Storm drain Landfill	Brånäsaldalen landfill	41,18	
77	2023-104-025	Urban Water - Storm drain Landfill	Brånäsaldalen landfill	40,87	
78	2023-104-024	Urban Water - Storm drain Landfill	Brånäsaldalen landfill	40,69	
79	2023-077-039	Urban Water - River	Nitelva Downstream landfill	39,04	
80	2023-077-041	Urban Water - Storm drain Landfill	Brånäsaldalen landfill	38,17	
81	2023-104-002	Urban Water - Storm drain Landfill	Brånäsaldalen landfill	37,99	
82	2023-104-048	Urban Water - Storm drain Landfill	Brånäsaldalen landfill	37,65	
83	2023-109-020	Shallow Groundwater	Well - Greece	37,49	
84	2023-077-038	Urban Water - River	Sagelva river Downstream	37,32	
85	2023-104-003	Urban Water - Storm drain Landfill	Brånäsaldalen landfill	36,75	
86	2023-077-057	Urban Water - River	Nitelva Outlet	35,57	

87	2023-077-082	Urban water - River	Nitelva Outlet Landfill	35,45	
88	2023-104-068	Urban Water - River	Nitelva outlet landfill	35,16	
89	2023-077-056	Urban Water - Storm drain Landfill	Brånásdalen landfill	35,09	
90	2023-135-003	Groundwater - Monitoring well	GLT/Horisont Landfill	33,90	
91	2023-077-069	Urban Water - Storm drain Landfill	Brånásdalen landfill	31,99	
92	2023-104-009	Urban Water - Storm drain Landfill	Brånásdalen landfill	31,80	
93	2023-077-098	Urban Water - Storm drain Landfill	Brånásdalen landfill	30,76	
94	2023-077-070	Urban Water - Storm drain Landfill	Brånásdalen landfill	29,66	
95	2023-077-058	Urban water - River	Sagelva Downstream	29,09	
96	2023-077-002	Urban Water - River	Glomma Fetsund	28,13	
97	2023-077-099	Urban water - River	Nitelva Outlet Landfill	27,08	
98	2023-077-077	Urban Water - Storm drain Landfill	Brånásdalen landfill	27,05	
99	2023-077-026	Urban Water - storm drain landfill	Brånásdalen landfill storm drain surface water	26,68	
100	2023-104-006	Urban Water - Storm drain Landfill	Brånásdalen landfill	25,51	
101	2023-077-096	Urban Water - Storm drain Landfill	Brånásdalen landfill	24,74	
102	2023-077-055	Urban Water - Storm drain Landfill	Brånásdalen landfill	24,38	
103	2023-077-012	Urban Water	Brånásdalen landfill storm drain surface water	24,34	
104	2023-077-021	Urban Water - storm drain landfill	Brånásdalen landfill storm drain surface water	23,67	
105	2023-104-015	Urban water - River	Nitelva Outlet Landfill	22,70	
106	2023-104-029	Urban Water - Storm drain Landfill	Brånásdalen landfill	22,63	
107	2023-104-045	Urban Water - River	Nitelva outlet landfill	22,30	
108	2023-104-053	Urban Water - Storm drain Landfill	Brånásdalen landfill	22,07	
109	2023-077-022	Urban Water - storm drain landfill	Brånásdalen landfill storm drain surface water	21,15	
110	2023-077-061	Urban Water - River	Nitelva	20,68	
111	2023-077-084	Urban Water - Storm drain Landfill	Brånásdalen landfill	20,30	
112	2023-077-037	Urban Water - River	Nitelva river Upstream	20,04	
113	2023-077-013	Urban Water	Brånásdalen landfill storm drain surface water	19,89	
114	2023-104-065	Urban Water - River	Rømua	19,62	
115	2023-077-007	Urban Water	Brånásdalen landfill storm drain surface water	19,09	
116	2023-077-011	Urban Water	Brånásdalen landfill storm drain surface water	18,93	
117	2023-104-050	Urban Water - Storm drain Landfill	Brånásdalen landfill	18,91	
118	2023-135-019	Groundwater - Monitoring well	GLT/Horisont Landfill	18,82	
119	2023-077-030	Urban Water - storm drain landfill	Brånásdalen landfill storm drain surface water	17,73	
120	2023-077-005	Urban Water	Nitelva Upstream	16,24	
121	2023-077-029	Urban Water - storm drain landfill	Brånásdalen landfill storm drain surface water	16,09	
122	2023-077-006	Urban Water	Nitelva Outlet	16,09	
123	2023-077-080	Urban Water - Storm drain Landfill	Brånásdalen landfill	15,74	
124	2023-077-044	Urban Water - Storm drain Landfill	Brånásdalen landfill	15,64	
125	2023-104-028	Urban Water - Storm drain Landfill	Brånásdalen landfill	15,60	
126	2023-077-066	Urban Water - Storm drain Landfill	Brånásdalen landfill	15,48	
127	2023-104-032	Urban Water - Storm drain Landfill	Brånásdalen landfill	15,43	
128	2023-077-010	Urban Water	Brånásdalen landfill storm drain surface water	15,21	
129	2023-104-023	Urban water - River	Sagelva downstream	14,80	
130	2023-077-046	Urban Water - Storm drain Landfill	Brånásdalen landfill	14,68	
131	2023-077-075	Urban Water - Storm drain Landfill	Brånásdalen landfill	14,67	
132	2023-104-033	Urban Water - Storm drain Landfill	Brånásdalen landfill	14,49	
133	2023-077-019	Urban Water	Brånásdalen landfill storm drain surface water	14,23	
134	2023-077-028	Urban Water - storm drain landfill	Brånásdalen landfill storm drain surface water	14,12	
135	2023-077-078	Urban Water - Storm drain Landfill	Brånásdalen landfill	14,08	
136	2023-104-018	Urban water - River	Sagelva Downstream	14,08	
137	2023-077-097	Urban Water - Storm drain Landfill	Brånásdalen landfill	13,88	
138	2023-104-016	Urban water - River	Sagelva Upstream	13,75	
139	2023-077-043	Urban Water - Storm drain Landfill	Brånásdalen landfill	13,66	
140	2023-135-011	Groundwater - Monitoring well	GLT/Horisont Landfill	13,62	
141	2023-104-057	Urban Water - Storm drain Landfill	Brånásdalen landfill	13,60	
142	2023-104-036	Urban water - River	Rømua river	13,57	
143	2023-104-041	Urban Water - River	Rømua river	13,41	
144	2023-135-009	Groundwater - Monitoring well	GLT/Horisont Landfill	13,32	
145	2023-077-024	Urban Water - storm drain landfill	Brånásdalen landfill storm drain surface water	13,27	
146	2023-077-079	Urban Water - Storm drain Landfill	Brånásdalen landfill	13,21	
147	2023-077-087	Urban Water - Storm drain Landfill	Brånásdalen landfill	13,09	
148	2023-077-003	Urban Water - River	Leira Downstream	13,09	
149	2023-077-004	Urban Water	Nitelva Downstream	12,75	
150	2023-077-040	Urban Water - River	Leiraelva Downstream	12,64	
151	2023-077-063	Urban Water - River	Nitelva Outlet Landfill	12,61	
152	2023-104-030	Urban Water - Storm drain Landfill	Brånásdalen landfill	12,59	
153	2023-077-053	Urban Water - Storm drain Landfill	Brånásdalen landfill	12,21	
154	2023-104-010	Urban Water - Storm drain Landfill	Brånásdalen landfill	11,68	
155	2023-104-055	Urban Water - Storm drain Landfill	Brånásdalen landfill	11,45	
156	2023-104-054	Urban Water - Storm drain Landfill	Brånásdalen landfill	11,29	
157	2023-104-014	Urban Water - Storm drain Landfill	Brånásdalen landfill	11,06	
158	2023-104-052	Urban Water - Storm drain Landfill	Brånásdalen landfill	10,74	
159	2023-104-013	Urban Water - Storm drain Landfill	Brånásdalen landfill	10,45	
160	2023-077-014	Urban Water	Brånásdalen landfill storm drain surface water	9,56	
161	2023-077-018	Urban Water	Brånásdalen landfill storm drain surface water	8,98	
162	2023-077-094	Urban Water - Storm drain Landfill	Brånásdalen landfill	8,70	
163	2023-104-011	Urban Water - Storm drain Landfill	Brånásdalen landfill	8,57	
164	2023-104-064	Urban Water - River	Leira Downstream	8,50	
165	2023-077-074	Urban Water - Storm drain Landfill	Brånásdalen landfill	8,45	
166	2023-104-058	Urban Water - Storm drain Landfill	Brånásdalen landfill	8,35	
167	2023-077-068	Urban Water - Storm drain Landfill	Brånásdalen landfill	8,33	
168	2023-077-036	Urban Water - River	Nitelva river Outlet Landfill	8,31	
169	2023-077-073	Urban Water - Storm drain Landfill	Brånásdalen landfill	8,31	
170	2023-077-052	Urban Water - Storm drain Landfill	Brånásdalen landfill	8,09	
171	2023-104-026	Urban Water - Storm drain Landfill	Brånásdalen landfill	7,97	
172	2023-077-017	Urban Water	Brånásdalen landfill storm drain surface water	7,90	
173	2023-104-043	Urban Water - River	leiraelva downstream	7,89	
174	2023-104-038	Urban water - River	Leiraelva downstream	7,83	
175	2023-077-051	Urban Water - Storm drain Landfill	Brånásdalen landfill	7,65	
176	2023-104-020	Urban water - River	Nitelva	7,59	
177	2023-104-042	Urban water - River	Leiraelva upstream	7,47	
178	2023-104-017	Urban water - River	Nitelva	7,35	
179	2023-077-035	Urban Water - storm drain landfill	Brånásdalen landfill storm drain surface water	7,24	
180	2023-104-034	Urban Water - Storm drain Landfill	Brånásdalen landfill	7,20	

181	2023-104-039	Urban Water - River	Leiraelva upstream	7,11	
182	2023-077-033	Urban Water - storm drain landfill	Brånåsdalen landfill storm drain surface water	6,91	
183	2023-104-066	Urban Water - River	Sagelva downstream	6,85	
184	2023-104-007	Urban Water - Storm drain Landfill	Brånåsdalen landfill	6,79	
185	2023-077-072	Urban Water - Storm drain Landfill	Brånåsdalen landfill	6,75	
186	2023-077-034	Urban Water - storm drain landfill	Brånåsdalen landfill storm drain surface water	6,68	
187	2023-077-065	Urban Water - River	Nitelva Downstream landfill	6,62	
188	2023-077-032	Urban Water - storm drain landfill	Brånåsdalen landfill storm drain surface water	6,59	
189	2023-077-015	Urban Water	Brånåsdalen landfill storm drain surface water	6,48	
190	2023-069-009	Lake Water	Lilledalstjernet lake	6,45	
191	2023-077-085	Urban Water - Storm drain Landfill	Brånåsdalen landfill	6,45	
192	2023-077-001	Urban Water - River	Sagelva Downstream	6,44	
193	2023-077-023	Urban Water - storm drain landfill	Brånåsdalen landfill storm drain surface water	6,42	
194	2023-077-071	Urban Water - Storm drain Landfill	Brånåsdalen landfill	6,37	
195	2023-104-059	Urban Water - Storm drain Landfill	Brånåsdalen landfill	6,34	
196	2023-077-076	Urban Water - Storm drain Landfill	Brånåsdalen landfill	6,33	
197	2023-077-049	Urban Water - Storm drain Landfill	Brånåsdalen landfill	6,30	
198	2023-077-016	Urban Water	Brånåsdalen landfill storm drain surface water	6,25	
199	2023-104-008	Urban Water - Storm drain Landfill	Brånåsdalen landfill	5,93	
200	2023-104-060	Urban Water - Storm drain Landfill	Brånåsdalen landfill	5,81	
201	2023-069-027	Lake Water	Bongsatjørna lake	5,78	
202	2023-104-019	Urban water - River	Nitelva downstream	5,59	
203	2023-104-051	Urban Water - Storm drain Landfill	Brånåsdalen landfill	5,50	
204	2023-077-050	Urban Water - Storm drain Landfill	Brånåsdalen landfill	5,36	
205	2023-077-025	Urban Water - storm drain landfill	Brånåsdalen landfill storm drain surface water	5,21	
206	2023-077-059	Urban Water - River	Sagelva Downstream	5,15	
207	2023-104-061	Urban Water - Storm drain Landfill	Brånåsdalen landfill	5,15	
208	2023-069-042	Lake Water	Småholmvatnet lake	5,00	
209	2023-077-060	Urban water - River	Sagelva Upstream	4,86	
210	2023-104-022	Urban water - River	Nitelva downstream landfill	4,63	
211	2023-104-021	Urban water - River	Nitelva Upstream	4,59	
212	2023-104-070	Urban Water - River	Nitelva downstream	4,52	
213	2023-104-067	Urban Water - River	Nitelva upstream	4,34	
214	2023-077-048	Urban Water - Storm drain Landfill	Brånåsdalen landfill	4,30	
215	2023-069-047	Lake Water	Dalbergvatnet lake	3,90	
216	2023-104-062	Urban Water - Tap Water	Tapwater from gas collection house	3,73	
217	2023-077-031	Urban Water - storm drain landfill	Brånåsdalen landfill storm drain surface water	3,61	
218	2023-077-095	Urban Water - Storm drain Landfill	Brånåsdalen landfill	3,52	
219	2023-077-067	Urban Water - Storm drain Landfill	Brånåsdalen landfill	3,28	
220	2023-069-025	Lake Water	Øvre Bergsvatnet lake	3,26	
221	2023-069-022	Lake Water	Kringlevatnet lake	3,22	
222	2023-069-064	Lake Water	Øygardstjørna lake	3,19	
223	2023-104-069	Urban Water - River	Glomma with Sorumsand	2,95	
224	2023-069-004	Lake Water	Lisle Frøysvatnet lake	2,92	
225	2023-104-044	Urban water - River	Glomma upstream	2,84	
226	2023-104-040	Urban water - River	Glomma downstream	2,82	
227	2023-104-031	Urban Water - Storm drain Landfill	Brånåsdalen landfill	2,73	
228	2023-104-035	Urban Water - River	Glomma downstream	2,65	
229	2023-069-059	Lake Water	Langtjernet lake	2,64	
230	2023-104-037	Urban Water - River	Glommsa upstream	2,61	
231	2023-077-062	Urban water - River	Leiraelva Downstream	2,59	
232	2023-104-063	Lake Water	Velmunden	2,57	
233	2023-069-060	Lake Water	Randsfjorden lake	2,53	
234	2023-077-042	Urban Water - Storm drain Landfill	Brånåsdalen landfill	2,51	
235	2023-069-038	Lake Water	Sandtjern lake	2,48	
236	2023-069-063	Lake Water	Midtvatnet lake	2,47	
237	2023-069-010	Lake Water	Tretjernet lake	2,44	
238	2023-069-052	Lake Water	Femvatnan lake	2,44	
239	2023-069-039	Lake Water	Bogatjørna lake	2,33	
240	2023-104-012	Urban Water - Storm drain Landfill	Brånåsdalen landfill	2,06	
241	2023-069-034	Lake Water	Vassdalsvatnet lake	2,05	
242	2023-104-056	Urban Water - Storm drain Landfill	Brånåsdalen landfill	1,97	
243	2023-069-041	Lake Water	Okstjørna lake	1,92	
244	2023-069-043	Lake Water	Småholmvatnet lake	1,85	
245	2023-069-026	Lake Water	Vongsatjørne lake	1,72	
246	2023-069-024	Lake Water	Kringlevatnet lake	1,56	
247	2023-069-005	Lake Water	Brekkevatnet lake	1,51	
248	2023-069-007	Lake Water	Holmevatnet lake	1,42	
249	2023-069-054	Lake Water	Femvatnan lake	1,29	
250	2023-069-053	Lake Water	Femvatnan lake	1,26	
251	2023-069-014	Lake Water	Øyyvatnet lake	1,24	
252	2023-069-036	Lake Water	Litleholtvatnet lake	1,21	
253	2023-069-017	Lake Water	Trytjørn lake	1,18	
254	2023-069-061	Lake Water	Fundsjøen lake	1,14	
255	2023-069-044	Lake Water	Småholmvatnet lake	1,13	
256	2023-069-058	Lake Water	Brumundsjøen lake	1,13	
257	2023-069-033	Lake Water	Jakobsvatnet lake	1,08	
258	2023-069-002	Lake Water	Korstjernet lake	1,05	
259	2023-069-019	Lake Water	Beritsjøni lake	1,03	
260	2023-069-048	Lake Water	Femvatnan lake	1,03	
261	2023-069-051	Lake Water	Femvatnan lake	0,93	
262	2023-069-056	Lake Water	Store Sorksjøen lake	0,93	
263	2023-069-023	Lake Water	Kringlevatnet lake	0,91	
264	2023-069-028	Lake Water	Bongsatjørna lake	0,81	
265	2023-069-035	Lake Water	Vassdalsvatnet lake	0,77	
266	2023-069-040	Lake Water	Fiskløysa lake	0,74	
267	2023-069-006	Lake Water	Rundatjørn lake	0,74	
268	2023-069-018	Lake Water	Grunntjørn lake	0,70	
269	2023-069-015	Lake Water	Øyyvatnet lake	0,65	
270	2023-069-062	Lake Water	Fundsjøen lake	0,61	
271	2023-069-021	Lake Water	Beritsjøni lake	0,56	
272	2023-069-037	Lake Water	Monstjørna lake	0,54	
273	2023-069-057	Lake Water	Mjølssjøen lake	0,54	
274	2023-069-029	Lake Water	Bongsatjørna lake	0,53	

275	2023-069-020	Lake Water	Beritstjørni lake	0,52	
276	2023-069-045	Lake Water	Smáholmvatnet lake	0,49	
277	2023-069-011	Lake Water	Gråtjørna lake	0,47	
278	2023-069-003	Lake Water	Korstjernet lake	0,46	
279	2023-069-046	Lake Water	Dalbergvatnet lake	0,42	
280	2023-069-055	Lake Water	Lyngen lake	0,37	
281	2023-069-030	Lake Water	Bongsatjørna lake	0,36	
282	2023-069-013	Lake Water	Sjugurdindtjørni lake	0,35	
283	2023-069-031	Lake Water	Bongsatjørna lake	0,31	
284	2023-069-001	Lake Water	Korstjernet lake	0,28	
285	2023-069-016	Lake Water	Butjørni lake	0,28	
286	2023-069-032	Lake Water	Bongsatjørna lake	0,26	
287	2023-069-049	Lake Water	Femvatnan lake	0,23	
288	2023-069-012	Lake Water	Halvorstjørna lake	0,22	

## Appendix C – Precision of The Method

**Table V3** – Raw data showing the precision of the method as reflected by the standard deviation between replicates.

Number of samples	ID	Date analyzed	Sample type	Recovery (%)	$\delta_{11B}$	Reference material used for delta correction	SD
1	2023-074-002	17/04/2024	Groundwater	30	9,72	AE120, AE121, AE122	2,52
1	2023-074-002	05/04/2024	Groundwater	11	6,16	AE120, AE121, AE122	
2	2023-109-042	10/01/2024	Seawater	344	35,38	AE120, AE121, AE122	6,48
2	2023-109-042	10/01/2024	Seawater	67	32,53	AE120, AE121, AE122	
2	2023-109-042	20/03/2024	Seawater	15	44,91	AE120, AE121, AE122	
3	2023-126-011	05/04/2024	Landfill Leachate	33	5,86	AE120, AE121, AE122	1,40
3	2023-126-011	17/04/2024	Landfill Leachate	71	7,84	AE120, AE121, AE122	
4	2023-126-012	05/04/2024	Landfill Leachate	32	4,59	AE120, AE121, AE122	3,49
4	2023-126-012	17/04/2024	Landfill Leachate	13	9,52	AE120, AE121, AE122	
5	2023-135-020	05/04/2024	Landfill Leachate	9	0,66	AE120, AE121, AE122	4,87
5	2023-135-020	17/04/2024	Landfill Leachate	79	7,55	AE120, AE121, AE122	
6	2023-136-001	10/01/2024	Seawater	78	38,84	AE120, AE121, AE122	12,75
6	2023-136-001	20/03/2024	Seawater	17	43,10	AE120, AE121, AE122	
6	2023-136-001	05/04/2024	Seawater	13	66,34	AE120, AE121, AE122	
6	2023-136-001	17/04/2024	Seawater	62	41,29	AE120, AE121, AE122	
7	2023-138-004	05/04/2024	Landfill Leachate	15	9,76	AE120, AE121, AE122	1,13
7	2023-138-004	17/04/2024	Landfill Leachate	7	11,37	AE120, AE121, AE122	
8	AE120	20/03/2024	Reference material	142	-17,53	AE120, AE121, AE122	2,21
8	AE120	17/04/2024	Reference material	89	-20,16	AE120, AE121, AE122	
8	AE120	05/04/2024	Reference material	12	-22,93	AE120, AE121, AE122	
8	AE120	10/01/2024	Reference material		-20,04	AE120, AE121, AE122	
9	AE121	20/03/2024	Reference material	155	14,25	AE120, AE121, AE122	3,74
9	AE121	17/04/2024	Reference material	87	19,77	AE120, AE121, AE122	
9	AE121	05/04/2024	Reference material	19	23,34	AE120, AE121, AE122	
9	AE121	10/01/2024	Reference material		19,43	AE120, AE121, AE122	
10	AE122	17/04/2024	Reference material	74	39,79	AE120, AE121, AE122	2,25
10	AE122	20/03/2024	Reference material	11	42,68	AE120, AE121, AE122	
10	AE122	10/01/2024	Reference material		40,01	AE120, AE121, AE122	
10	AE122	05/04/2024	Reference material	176	37,19	AE120, AE121, AE122	
11	AE122 2	26/04/2024	Reference material	25	36,77	No correction due to too low concentration	2,87
11	AE122 2	01/03/2024	Reference material	69	40,83	No correction due to too high blank	
12	AE123	17/04/2024	Reference material	69	2,25	AE120, AE121, AE122	10,42
12	AE123	05/04/2024	Reference material	13	-12,49	AE120, AE121, AE122	
13	NIST951a	01/03/2024	Reference material	91	-5,98	No correction due to too high blank	2,62
13	NIST951a	01/03/2024	Reference material	94	-3,16	No correction due to too high blank	
13	NIST951a	01/03/2024	Reference material	91	-0,75	No correction due to too high blank	

## Appendix D – Column Lifetime Raw Data

**Table V4** – Table showing the column lifetime raw data.

<b>n</b>	<b>ID</b>	<b>Sample</b>	<b>Actual concentration (ng/mL)</b>	<b>Measured concentration (ng/mL)</b>	<b>Recovery</b>	<b>Delta</b>	<b>Signal/noise</b>
1	2023-136-001 1	12	34	17	52	31,90	4,22
2	2023-136-001 2	23	34	16	49	31,91	5,19
3	2023-136-001 3	36	34	18	54	32,48	5,13
4	2023-136-001 4	47	34	18	53	31,74	5,06
5	2023-136-001 5	60	34	18	52	32,10	5,20
6	2023-136-001 6	71	34	17	49	32,06	5,33
7	2023-136-001 7	84	34	8	23	33,12	5,97
8	2023-136-001 8	95	34	9	26	32,27	6,77
9	2023-136-001 9	108	34	8	23	33,43	4,67
10	2023-136-001 10	119	34	7	21	36,35	5,88
11	2023-136-001 11	132	34	18	53	31,64	5,61
12	2023-136-001 12	143	34	12	36	34,10	3,87

## Appendix E – pH Effect on Recovery

**Table V5** - Measured pH and recovery on a seawater sample that underwent prepFAST separation with varying ratios of HNO<sub>3</sub>, Milli-Q water, ammonium acetate and the seawater sample from the North Sea (2023-136-001). The final concentration of the seawater sample is 144 ng/mL and the original concentration was 5750 ng/mL.

n	Ammonium acetate 4 mol/L (μL)	HNO <sub>3</sub> 2 mol/L (μL)	MQ-H <sub>2</sub> O (μL)	2023-136-001 (μL)	Recovery of atomic boron	pH
1	2000	500	1400	100	100	5,4
2	1800	450	1650	100	100	5,38
3	1600	400	1900	100	100	5,33
4	1400	350	2150	100	100	5,32
5	1200	300	2400	100	100	5,29
6	1000	250	2650	100	100	5,27
7	800	200	2900	100	100	5,24
8	600	150	3150	100	100	5,19
9	400	100	3400	100	100	5,14
10	200	50	3650	100	100	5
11	0	0	3900	100	100	2,22 <sup>2</sup>
12	2000	500	1500	0	100	5,37
13	1000	250	2750	0	100	5,21
14	0	0	4000	0	100	6,5

<sup>2</sup> This sample only consists of seawater and Milli-Q water. The low pH of 2.22 indicates some type of error in this measurement.



**Norges miljø- og biovitenskapelige universitet**  
Noregs miljø- og biovitenskapelege universitet  
Norwegian University of Life Sciences

Postboks 5003  
NO-1432 Ås  
Norway